INVESTIGATION OF THE STRUCTURE OF THE ELECTROMAGNETIC FIELD AND RELATED PHENOMENA, GENERATED BY THE "ACTIVE" SATELLITE

Grant NAG5-1340

SEMIANNUAL REPORT N°2

For the period November 1, 1990 through April 30, 1991

Principal Investigator

Dr. Yakov L. Alpert

July 1991

Prepared for
National Aeronautics and Space Administration
Greenbelt, Maryland 20771

Smithsonian Institution
Astrophysical Observatory
Cambridge, Massachusetts 02138

The Smithsonian Astrophysical Observatory
is a member of the
Harvard-Smithsonian Center for Astrophysics

The NASA Technical Officer for this grant is Mr. Paul Pashby, Code 602
Goddard Space Flight Center, Greenbelt, Maryland 20771.

Contents

Abstract

The altitude dependencies of the *moduli of the electric field* E in the VLF and LF frequency bands ($F_B \ll F < f_B$) and in the altitude range of the ionosphere $Z = (400\ to\ 2500)\ km$ up to $Z = 6000\ km$ (the bottom of the magnetosphere) were calculated by the linear theory. The amplitudes of the field have large maxima in four regions: the Axis field $|E_0|$ close to the direction of the Earth's magnetic field line $\mathbf{B_0}$, $\beta \sim 0$ degrees, the fields $|E_{St}|$, $|E_{RevSt}|$ and $|E_{Res}|$ in the Storey, Reversed Storey and Resonance cones, $\beta \sim (0 \rightarrow 20)$ *degrees*. Their maxima are very pronounced close to the low hybrid frequency F_L. Especially large one is the enhancement of the Axis field $|E_0|$ at $Z \geq (1000 - 2500)\ km$. It grows up for about 10^6 times in this region and it is concentrated in very small angles $\Delta\beta < 1$ *degree*. The spatial distribution of $|E_0|$ becomes similar to a laser beam.

The *nonlinear heating of a magnetoplasma* under the action of an electric field $Ee^{i\omega t}$ is recently expanded by the microscopic theory by the author. The velocities, collision frequencies and temperatures of all the constituents of a magnetoplasma - electrons, ions and neutral particles - are taken into account. Formulae and numerical results, particularly obtained by a computer, are presented for the ionosphere in the frequency band $F = (1\ to\ 10^4)\ kHz$ and altitude range $Z \simeq (100 - 1000)\ km$. The temperatures are growing up very quickly with altitude and reach at $Z \sim (150 - 200)\ km$ the ionization potential even when the electric field E is about some units of mv/m. At these altitudes $T_e \geq 10^2 \cdot T_{n0}$. Some results of calculations by the self consistent solution of the basic system of equations are also discussed.

I. Introduction

The proposal P2159-8-89 for the grant NAG5-1340 mainly envisaged theoretical study:

of the structure of the electromagnetic field in the ionosphere at altitudes $(500 - 2500)\ km$ in the frequency band $F = (1 - 16)\ kHz$ generated by the PVP Transmitter of the Sub- satellite of the Active System;

and of the heating (temperatures) of the surrounding magnetoplasma under the action of the radiation of the powerful VLF generator, $F \simeq 10\ kHz$ of the Active Satellite.

Besides it was supposed that the study of this two problems will be done for realistic models of the ionosphere, based on measurements performed by the Active System. So, the main task of this proposal was theoretical treatment of experimental data. The proposal was for 2 years for the period of October 1, 1989 through September 1991 and was officially approved by NASA in December 1989.

However, because of the failure and delayed launch of the Active Satellite and of the Sub- satellite by the USSR and Czechoslovakia, the term of this proposal was shortened to the period of one year. The author had to change the programme of the theoretical calculations. In general, the study of this problem in more detail remains very important and interesting both for this field and because these results can and will be used in the future by more successful launches of a system of two satellites with an improved programme, similar to the Active mission, what should be done by NASA indeed.

Following to the main task of the proposal, the study of the structure of the electric field was extended for a wider band of frequencies $F \sim (1\ to\ 30-40)\ kHz$, and a wider range of altitudes up to $Z \sim 6000\ km$. The

study of the structure of the electric field at higher altitude is very important because the trajectory of propagation of ELF, VLF and LF electromagnetic waves in the magnetosphere are passing close to the Earth's magnetic field lines. The author believes to extend these calculations up to the apogee of the magnetic field lines (tens of 1000 km) in the next study. Besides, we restricted ourselves to learn in detail only the, so called, "Axis field" $|E_0|$, i.e. close to the direction of the magnetic field $\mathbf{B_0}$. This is the most important and new peculiarity of the problem learned by Alpert, Budden and Moiseyev (see [2] to [5]). Namely the theoretical basis of these papers was used in this report. These calculations were done by the computer of the Goddard Flight Center in collaboration with James Green and Lara Aist-Sagara.

The recently extended by the author microscopic theory was used for the calculations of the heating under the action of the electric field of the Magnetoplasma - of the temperatures of the ionosphere. By theoretical investigation of the parametric and nonlinear phenomena, which could be produced in the Tethered Magnetospheric Cloud (see [6]), the author had specially widened the theory, keeping in mind the interest to learn these phenomena in a broader altitude range than the altitude of the Tether System $Z = 300\ km$ (see also [7], [8]). The main part of the presented here results of calculations were done by the computer and program composed by Robert Estes. They are given in the following sections.

II. Altitude and frequency dependencies of the electric field $|E|$ of e.m. waves in the ionosphere $Z = (400\ to\ 6000)\ km$.

The altitude dependences of the moduli of electrical fields $|E|$ were calculated for the model of the inosphere given in Table I. This model is nearly conformed to the conditions of the day-time middle altitude ionosphere. The notations used in the table and below in the paper are:

Z is the altitude above the Earth's surface, N_n and $N_{e,i}$ are the densities of the neutral particles, electrons and ions;

$T°K$ and B, γ are the temperature in Kelvin degrees and the magnetic field in gammas $\gamma(nT)$ along the Earth's magnetic field line;

ν_{en} and ν_{ei} are the collision frequencies between the electrons and the neutral particles and the ions;

f_0 and F_0 are the Lengmuir plasma frequencies of the electrons and ions;

f_B, F_B, F_L are the electron's and ion's gyrofrequencies and the low hybrid frequency of the ions

$$F_L = \left(\frac{f_B F_B}{1 + \frac{f_B^2}{f_0^2}} \right)^{1/2} . \tag{1}$$

Up to the altitude about $(800 - 1000)\ km$ the ionosphere consists of a noticeable number of Oxygen and Helium ions (O_1^+ and He^+) including protons H_1^+. Therefore, in the lower part of the discussed region of the ionosphere, for calculations of the electron and ion gyrofrequencies f_B and F_B, the effective mass of the neutral particles is used:

$$M_{eff} = M_{H_1} \left(\sum_{s=1,2,3} \frac{N_{is}}{N_{ei}} \cdot \frac{M_{H_1}}{M_{is}} \right)^{-1} , \quad s = 1,2,3. \tag{2}$$

In (2), N_{is} and M_{is} are, respectively, the ion densities and masses of H_1^+, He^+ and O_1^+.

Table 1. Parameters of the ionosphere.

$Z\,, km$	300	400	500	800	1000	1500	2000	2500	3000	4000	6000
$N_n\,, cm^{-3}$	$3\cdot10^9$	$5\cdot10^8$	$5\cdot10^7$	$2\cdot10^6$	$4\cdot10^5$	$6\cdot10^3$	$2\cdot10^3$	20	<1	~0.2	$\ll1$
$N_e\cdot10^{-3}\,, cm^{-3}$	1800	1500	1000	400	230	70	20	10	8	6	5
M^+_{eff}/M^+_{H1}	5	3	2	1.2	1	1	-	-	-	-	-
$T\,, K^\circ$	1500	1800	1800	1800	2000	2500	3000	3500	4000	4500	5000
$B_0\cdot10^{-4}\,, \gamma$	4.37	4.15	3.96	3.52	3.24	2.66	2.21	1.82	1.55	1.15	0.68
$\nu_{en}\,, s^{-1}$	33	6	0.7	$3\cdot10^{-2}$	$8\cdot10^{-3}$	$6\cdot10^{-4}$	-	-	-	-	-
$\nu_{ei}\,, s^{-1}$	3000	1500	700	150	40	20	7	2	1.5	1	0.7
$f_0\cdot10^{-6}\,, Hz$	12.04	11.0	8.98	5.08	4.31	2.38	1.27	0.898	0.82	0.71	0.63
$F_0\cdot10^{-4}\,Hz$	12.57	14.8	14.8	12.1	10.1	5.55	2.96	2.09	1.91	1.65	1.45
$f_B\cdot10^{-5}\,, Hz$	12.25	11.62	11.1	9.87	9.07	7.45	6.21	5.09	4.34	3.21	1.91
$F_B\cdot10^{-2}\,, Hz$	1.33	2.1	3.02	4.47	4.93	4.05	3.38	2.77	2.36	1.74	1.04
$F_L\cdot10^{-3}\,Hz$	12.68	15.53	18.17	20.61	20.69	16.58	13.05	10.33	8.89	6.79	4.27

By the numerical calculations, presented in Section II.3, the altitude parameters of the magneroplasma given in Table I are used. In Section II.2, where a general view of all the cones and branches of the electric field is given, the conditional model of the ionosphere is the following:

$$\begin{aligned} f_0 &= 3.39 \cdot 10^6\ Hz,\ \ f_H = 1.194 \cdot 10^6\ Hz\ \ F_L = 2.49 \cdot 10^4\ Hz, \\ \nu_{ei} &= 10^{-2}\ sec^{-1},\ \ \frac{m}{M_{H_1}} = \frac{m}{M_{eff}} = 5.44 \cdot 10^{-4} \end{aligned} \tag{3}$$

II.1 Statement of the problem. Equations, formulae.

The linear theory of radiation of an electric dipole in a magnetoplasma, used in this study, was developed by Alpert, Moiseyev (1980 a,b, 1983), and Alpert, Budden, et al. (1983) (see [2] to [5]). The theoretical results of these papers, namely: the main formulae, the computer program and the general physical understanding of this problem, obtained in these studies, are used here for producing a picture of the expected structure of the electromagnetic field radiated in the neighborhood of a *mother satellite*, moving in the ionosphere at altitudes of the Active system. Besides it is supposed that this field is recorded on the far zone of this source by a *child sub-satellite*, moving around the mother satellite at distances from it $r \sim 10s$ *to* 100 *km* or a little more. Then the developed in the cited above papers theory for a homogeneous medium may be used for calculations of the electric field around the mother body, at the discussed here altitudes of the ionosphere and in the magnetosphere . This is a sufficiently good approximation because at the interesting for us altitudes, on such distances r from the mother body, the magnetosphere may be considered as a homogeneous medium. It is also supposed that the local parameters of the magnetoplasma (the electron and ion densities, the collision frequencies, the magnetic field, etc.) in the neighborhood of these bodies were estimated by this experiment simultaneously

with the recording of the amplitudes of the electric field.

An homogeneous cold non-magnetic magnetoplasma, which is characterized by a superimposed magnetic field, and by an electrical tensor ε_0 and a refractive index $\mathbf{n}$ is considered. The magnetic field is parallel to the $\mathbf{z}$ axis in the cartesian (x, y, z) and in the cylindrical (ρ, φ, z) coordinate systems. The refractive index may be thought by us as a vector $\mathbf{n}$ with components

$$\begin{aligned} n_x &= n \sin\Theta \cos\varphi, \quad n_y = n \sin\Theta \cdot \sin\varphi, \quad n_z = n \cos\Theta, \\ n_\varphi^2 &= (n_x^2 + n_y^2) = n^2 \sin^2\Theta, \end{aligned} \tag{4}$$

where Θ is the angle of the wave normal to the vector $\mathbf{k}$ with the $\mathbf{z}$ axis, $\mathbf{z} \parallel \mathbf{B_0}$. The electromagnetic waves $\mathbf{E}, \mathbf{H} \sim e^{i\omega t}$, generated in the magnetoplasma, are produced by an electric dipole of moment $\mathbf{I}e^{i\omega t}$, $\omega = 2\pi F$ is the angular frequency of the waves. The electric dipole is parallel to the $\mathbf{z}$ axis, i.e. $\mathbf{I} \parallel \mathbf{B_0}$. The source dipole is placed at $x = y = z = 0$, i.e. on the mother satellite. The receiving point is at a distance $r = \sqrt{x^2 + z^2}$ from the source in a direction β to the magnetic field $\mathbf{B_0}$ and

$$x = r \sin\beta, \quad y = 0, \quad z = r \cos\beta \tag{5}$$

since the plasma has rotational symmetry around the $\mathbf{z}$ axis.

The general solution of the system of the Maxwell equations of this problem is described by a sum of complicated integrals (see [2], [3]). The integrands of these integrals are rapidly oscillating functions. They are described by the Bessel functions $J_0\left(n_\perp, \frac{\omega}{c}\rho\right)$ and $J_1\left(n_\perp, \frac{\omega}{c}\rho\right)$, and the derivatives $\frac{dn_\parallel}{dn_\perp}$ where

$$n_\perp = n \sin\Theta, \quad n_\parallel = n \cos\Theta, \quad n^2 = n_\perp^2 + n_\parallel^2.$$

These integrals may be studied only by numerical methods. The method of the steepest descents, i.e. the stationary phase method was used for this

purpose. Certainly, the accuracy of this asymptotic method is sufficiently high only in the far zone from the source, namely, when

$$\frac{\omega}{c}\sqrt{\rho^2+z^2}=\frac{\omega}{c}r\gg 1. \tag{6}$$

The *main contribution* to the field is made by saddle points. Two cases should be considered by analyzing the integrals. Namely these cases characterize the basic physical properties of the field.

The first case is when the observation point - the receiver - is at very small horizontal distances from the source, namely, when $x\sim 0$, i.e. the angle β of the ray direction is very small. In this region the field is growing up and *becomes very strong* close to the direction of the magnetic field. It is called the *Axis field.* The saddle points are estimated in this case by the equation

$$\frac{dn_{\|}}{dn_{\perp}}=0 \tag{7}$$

The Axis field *enhancement* appears when $\omega>\omega_L$, ω_L is the low hybrid frequency. This is one of the most interesting peculiarities of this problem (see [1] and below). For many decades, an erroneous conclusion was in the literature that the field disappears close to the direction of the magnetic field $\mathbf{B_0}$ (see, for example, Arbel and Felson [5]).

The second important case is when $n_{\perp}\rho\gg 1$ and the observation point is sufficiently far from the axis, from the direction of the magnetic field $\mathbf{B_0}$. In this case, the asymptotic of the Bessel function

$$J_0, J_1\sim(2\pi n_{\perp}\rho)^{1/2}exp\left[-i\left(n_{\perp}\rho-\frac{\pi}{4}\right)\right] \tag{8}$$

may be used. The saddle points are estimated in this region by the equation

$$\cos\beta\frac{dn_{\|}}{dn_{\perp}}+\sin\beta=0 \tag{9}$$

The field is enhanced in the regions where two saddle points of the integrands are close to each other - they coalesce. Two regions of enhancement of the field exist in this case in different angle intervals β. They appear in the, so called, Storey and Reversed Storey cones. The field becomes especially strong in the Reversed Storey cone at frequencies $\omega < \omega_L$ (see [2] to [5]).

Certainly, one more region of the enhancement of the field is the *resonance cone*. It occurs when the coefficient of refraction $n \to 0$. At the resonance

$$\Theta - \beta = \pm\frac{\pi}{2}, \quad \tan^2\beta = -\frac{\varepsilon_{xx}}{\varepsilon_{zz}}, \tag{10}$$

where ε_{xx} and ε_{zz} are the elements of the tensor ε_0. In our case, the cartesian coordinates

$$\varepsilon_0 = \begin{bmatrix} \varepsilon_{xx} & \varepsilon_{xy} & 0 \\ \varepsilon_{yx} & \varepsilon_{yy} & 0 \\ 0 & 0 & \varepsilon_{zz} \end{bmatrix}, \quad \varepsilon_{xx} = \varepsilon_{yy} \tag{11}$$

The computer program used in the cited above paper by Alpert, Budden, etc. [3] for numerical calculations of the moduli $|E|$ of the electric field in the four regions of their enhancement, was developed by K. Budden, the formulae for the components of the electric field given in this paper were used. They remain complicated even by using of the first order descents evaluation of the integrals which gives the contribution to one saddle point of the Axis field $|E_0|$ and to two saddle points of the Storey $|E_{St}|$ and Reversed Storey $|E_{RevSt}|$ cones.

The field E_0 is expressed by an algebraic combination of the both Bessel functions $J_0(n_\perp, \rho)$ and $J_1(n_\perp, \rho)$ (see (5)), and also by a combination of the components of the refraction index **n** and of the elements of the tensor ε of the plasma. The fields $|E_{St}|$ and $|E_{RevSt}|$ are expressed by a combination of the Airy integral function $A_i(p)$ and its derivative $A_i'(p)$, and also by **n** and

ε_0. The field in the resonance cone $|E_{Res}|$ is much simpler and is expressed by an algebraic combination of the elements of the tensor, and the refraction index of the plasma. Certainly, all these formulae depend on the angular frequencies ω and the angle of the ray direction β.

For orientation the formulae used by the programming are given here only schematically. They give a general presentation about the distance, frequency and angle dependence of the interesting for us moduli of the field

$$|E| = \left(|E_x|^2 + |E_y|^2 + |E_z|^2\right)^{1/2} \tag{12}$$

These asymptotic formulae are of the following shape:

The Axis field

$$\begin{aligned} |E_0| \;\simeq\; & \left(I\frac{\omega^3}{c^3}\right) n_\rho^2 \left(\frac{2\pi n_z}{\frac{\omega}{c}z}\right)^{1/2} \cdot exp\left[-i\left(\frac{\omega}{c}zn_z \pm \frac{\pi}{4}\right)\right] \cdot \\ & \cdot \;\; F_{Ax}[J_0,\; J_1,\; \mathrm{n},\; \varepsilon_0], \end{aligned} \tag{13}$$

where all the values of $F_{Ax}[\ldots]$ depend on ω, β and on the characteristics frequencies of the magnetoplasma (see [2]).

The field in the two Storey cones

$$\begin{aligned} E_{St} \;\simeq\; & \left(I\frac{\omega^3}{c^3}\right) \cdot \frac{\sqrt{\pi} \cdot exp(-i\{\ldots\})}{\left(\frac{\omega}{c}r\right)^{5/6} \cdot (\cos\beta)^{1/3} \cdot (\sin\beta)^{1/2}} \cdot \\ & \cdot \;\; F_{St}\left[A_i(p),\; A_i'(p),\; \mathrm{n},\; \varepsilon_0\right], \end{aligned} \tag{14}$$

where all the values of $F_{St}[\ldots]$ depend on ω, β, etc., $A_i(p)$ and $A_i'(p)$ are the Airy function and its derivative,

$$p = \left(\frac{dn_{\|}}{dn_{\perp}} + \frac{\rho}{z}\right) \cdot \left(\frac{2}{n_{\|}}\right)^{1/2} \cdot \left(\frac{\omega}{c}z\right)^{2/3}, \tag{15}$$

and $\{...\}$ is determined by some parameters of the magnetoplasma, by ω and β (see [3]).

The field in the Resonance cone

$$|E_{Res}| \simeq \left(I\frac{\omega^3}{c^3}\right) \cdot \frac{n_\rho n_z exp\left[-i\frac{\omega}{c}r(n_\rho \sin\beta + n_z \cos\beta)\right]}{\left(\frac{\omega}{c}r\right)} \cdot \\ \cdot \quad F_{Res}\left[\mathbf{n}(\omega,\beta),\ \varepsilon_0(\omega,\beta),\ \beta\right]. \tag{16}$$

Let us note here the *sufficiently different dependence* of $|E_0|$, $|E_{St}|$, $|E_{RevSt}|$ and $|E_{Res}|$ on distance from the source.

II.2 Frequency dependence of $|E|$ in all regions-cones of their enhancement. General picture.

The distribution of the cones of the electrical field amplitude $|E|$ enhancement, formed in the magnetoplasma around the direction of the magnetic field $\mathbf{B_0}$, i.e. around the Axis field $|\mathbf{E_0}|$ in all the frequency bands is shown on Fig.1.

The generatix of the Storey cones containes the angles

$$\beta_M = (\beta_{St,M} \ \ to \ \ \beta_{St,0}), \tag{17}$$

where $\beta_{St,M}$ is the maximal value of β_M of the maxima of the angle dependence $\beta(\Theta)$, i.e of the direction of the group velocity $U = \frac{d\omega}{dk}$ of the wave. Let us remind that Θ is the angle between the wave vector $\mathbf{k}$ and the magnetic field $\mathbf{B_0}$. By both of these angles the $\beta(\Theta)$ dependences have points of inflection. The generatix of the Reversed Storey cone contains the angles of the minima of the dependence $\beta(\Theta)$, they are

$$\beta_m = (\beta_{St,m} \ \ to \ \ 0). \tag{18}$$

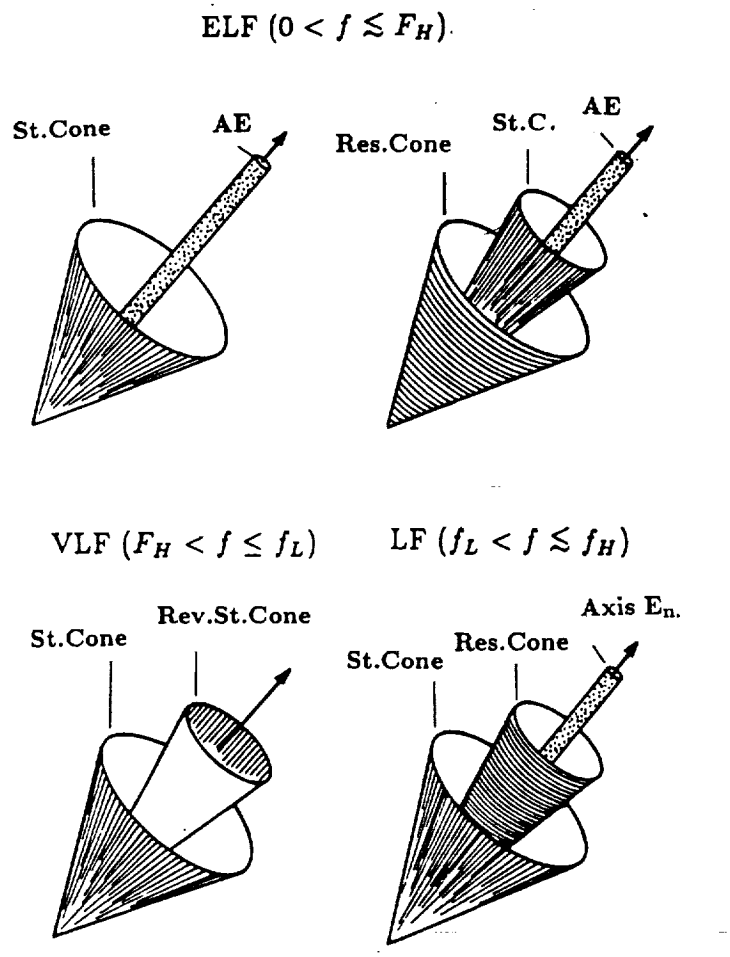

Fig 1. The regions (axis and cones) of enhancement of the electric fields moduli $|\mathbf{E}|$.

The frequency bands of these branches of waves are $F_M = (F_{St,M}\ to\ f_{SO})$ for the Storey cone and $F_m = (F_{St,M}\ to\ F_L)$ for the Reversed Storey cone. At the frequency $F_{St,M}$, where $F_B < F_{St,M} \ll F_L$, the Storey cones are combined (see below Fig.4 and [3], [4]). The frequency F_{S0} lies in the band of the electron whistler mode, $f_{S0} \leq f_B$. For the following in this section results of calculation of the fields $|E_{St}|$ and $|E_{RevSt}|$, these characteristic frequencies and angle $\beta_{St,M}$ are equal to:

$$\begin{aligned} F_{St,M} &= 2.6 \cdot 10^{-3} f_B, \quad \beta_{St,M} \sim 21°, \\ F_{St,0} &= 0.48 f_B, \quad F_B = 5.4 \cdot 10^{-4} f_B \end{aligned} \tag{19}$$

and F_B is the ion's gyrofrequency. The most important characteristic of the Storey cones fields is the large enhancement of $|E_{ResSt}|$ in the Reversed Storey cone by approaching the low hybrid frequency, namely, when

$$F_{St,m} \to F_L, \quad \beta_m \to 0. \tag{20}$$

The resonance cones are formed in the angle range $\beta_{Res} = (0\ to\ 90)°$ in the frequency band $F_L\ to\ f_B$.

The frequencies used in this study lie in the very low frequency band VLF, $F_B < F \leq F_L$ and in the low frequency band LF, $F_L < f < f_B$. By calculating of $|E|$ in the extra low frequency ELF, $0 < F < F_B$, the presence of ions of different kind should be taken into account. In general, the behavior of $|E|$ of ELF waves is the same, however, it becomes more complicated because of the presence of several ion gyrofrequencies, ion-ion hybrid frequencies and crossover frequencies (see [4], [5]). The angle and frequency dependencies of the moduli of the electric field $|E|$ of VLF and LF waves presented here for the model ionosphere, given above by (3), are shown on Figs. (2 to 4). Only two regions of enhancement of the field exist in the VLF

band. They are the branches $|E_{RevSt}|$ and $|E_{St}|$. Depending on β, they are oscillating when $F = const$ and are given on Fig.2 for $F = 10^{-2} f_B < F_L$. Three branches $|E_0|$, $|E_{St}|$ and $|E_{Res}|$ exist in the LF band. The field $|E_0|$ is also an oscillating function on β. Three fields are given on the same figure for $F_L < F = 10^{-2} f_H$. The angle dependence of $|E_{Res}|$ for different frequencies is shown on Fig.3 in more detail. It is seen that the values of the maxima $|E_{Res}|_{max}$ are changing sufficiently slow with frequency. However, by approaching the low hybrid frequency, the value of $|E_{Res}|_{max}$, similar to the $|E_{RevSt}|_{max}$ and $|E_0|_{max}$, is growing up very quickly: $|E_0|_{max}$ becomes about $10^3 - 10^5$ times larger by small changes of the frequency close to F_L. The shape of the frequency amplitudes of the electric field dependencies in this region is of resonance type. This is seen in more detail in the next section, where results of calculation of the Axis field E_0 are given.

Frequency dependencies of the maximal values of the moduli of the electric field $|E|_{max}$ in all the regions of their enhancement are shown on Fig.4. They are calculated for the model of the ionosphere given by (3).

II.3 Electric field $|E_0|$ nearby the Axis, direction z $\parallel$ B.

The behavior of the electric field around the source of radiation at different altitudes of the ionosphere is presented in this section by detailed calculation of the Axis field $|E_0|$. These results are presented here by the Figs. (5 to 10) and Table II. By calculation of $|E|$ in both this and previous section, the factor $\left(I\frac{\omega^3}{c^3}\right)$ is omitted (see formulae (5) to (9)). This factor is used only on one of the dependencies shown on Fig.10.

The oscillating character of $|E_0|$, depending on the horizontal distance x

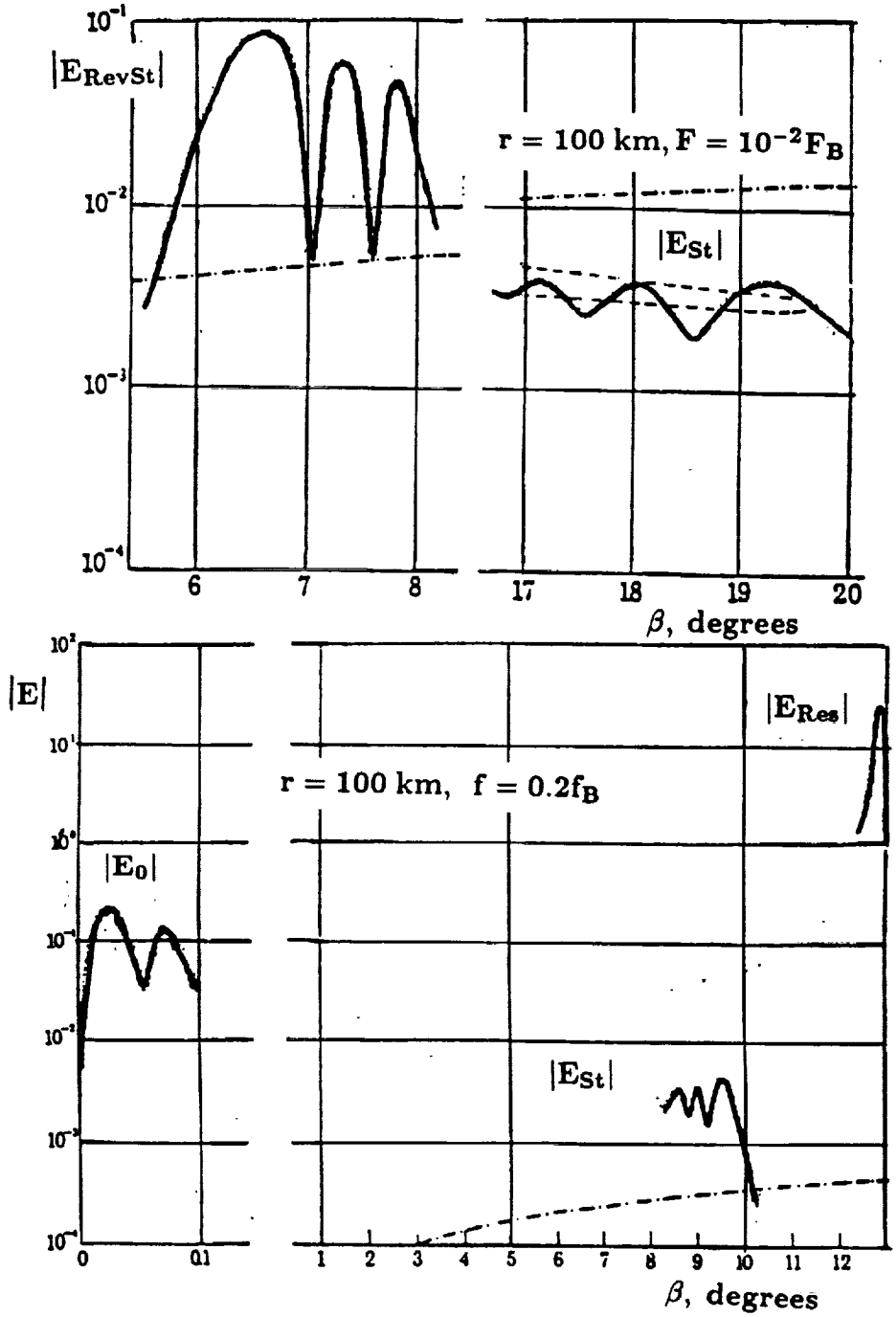

Fig 2. Angle dependencies of the moduli of the electric field $|E_0|$, $|E_{RevSt}|$ and $|E_{Res}|$ along the axis, in the Storey and Resonance cones.

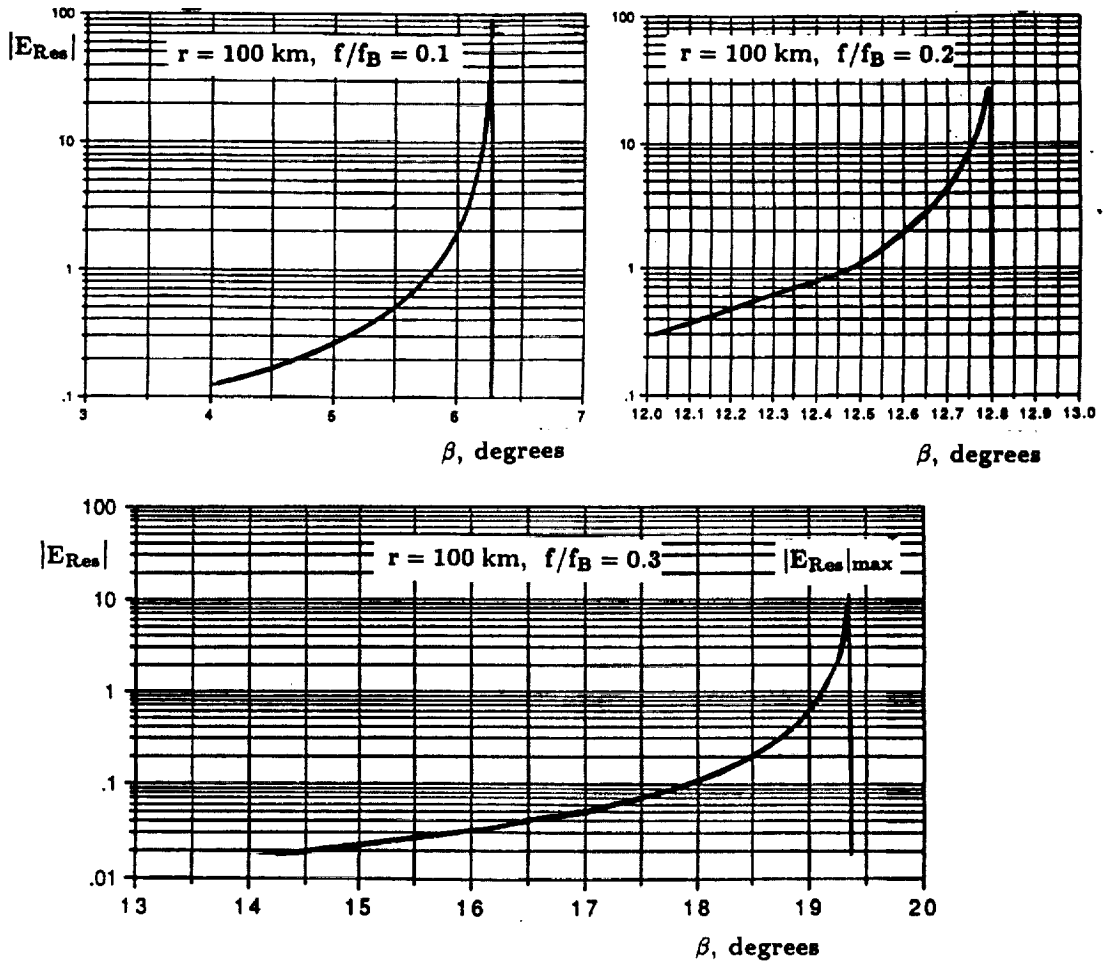

Fig 3. Angle dependencies of the electtic field moduli $|E_{Res}|$ in the Resonance cones at different frequencies far from f_L.

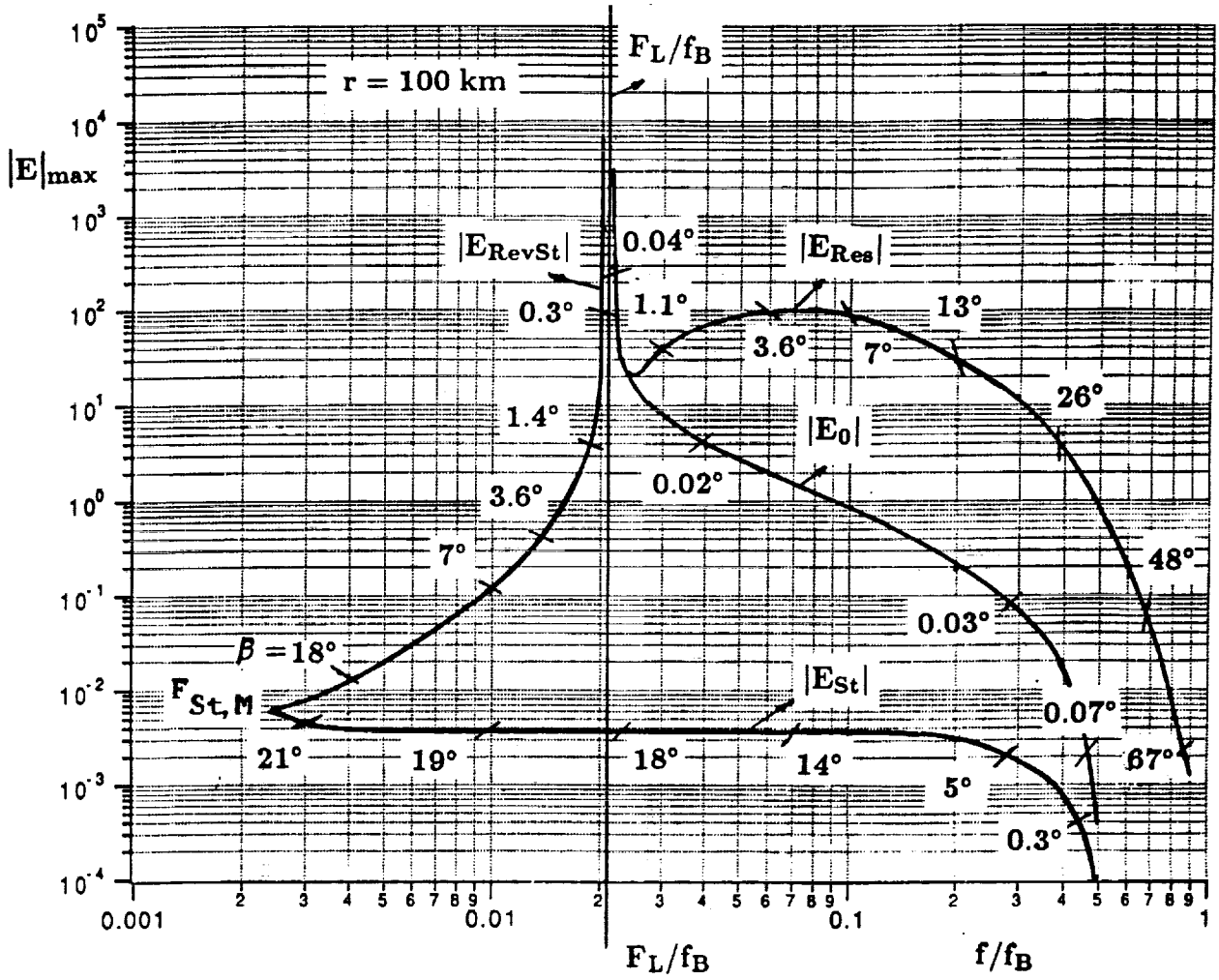

Fig 4. Frequency dependencies of the maximal values of the modulii $|E|_{max}$ of the electric fields in all the regions of their enhancement.

from the Axis **z**, i.e. from the direction of the magnetic field $\mathbf{B_0}$ at a distance r, $(x/r = \tan\beta)$ from the source is shown on Fig.5. Two important peculiarities of the field $|E_0|$ are seen at once by looking at these plots:

1. The amplitude is growing up very quickly especially in the altitude region $Z = (500\ to\ 800)\ km$.

2. The maximal values of $|E_0|_{max}$ are very close to the direction of $\mathbf{B_0}$, $x \ll 10^{-1}\ km$, $\beta \sim \frac{x}{r} \ll 0.1°$.

The frequency (F/f_B) dependencies of $Max|E_0|_{max}$, i.e. the maximal values of the maxima of $|E_0|_{max}$ (see Fig.5) at different altitudes are shown on Figs. 6 and 7. The asymmetric resonance-like, but of spiking shape of $|E_0|_{max}$ is especially very pronounced at $Z > 1000\ km$. By $Z = 2500\ km$ and $Z = 6000\ km$, the values of $|E_0|$ are changing $(10^3 - 10^4)$ times in very small intervals. In general, the amplitude at these altitudes is diminished for about $(10^5 - 10^6)$ times up to the more or less stabilized values of $|E_0|_{max}$. The angle dependencies $\beta(F)$ are illustrated on Figs. 8 and 9, where the $|E_0|_{max}$ dependencies are also shown. The spiking shape of $\beta(F)$ is similar to the shown of the frequency dependencies of $|E_0|_{max}$. The minimal values of $\beta(F)$ are very small, $\beta \ll 10^{-1}\ degrees$.

The result of calculations, presented on Figs. (6 to 9), are summarized on Fig.10 and Table II, where the altitude dependencies of $Max|E_0|_{max}$ and of its normalized value to $Z = 500\ km$

$$\delta|E_0|_{max} = \frac{(Max|E_0|_{max} \cdot F^3_{max})_Z}{(Max|E_0|_{max} \cdot F^3_{max})_{Z=500\ km}} \qquad (21)$$

are given. The frequencies F_{max} of the corresponding values of $Max|E_0|_{max}$ are also given in the table.

Table II.

Z , km	$\mathrm{Max}\lvert\mathbf{E_0}\rvert_{\max}$	$\mathrm{F_{max}}$ kHz	$\delta\lvert\mathbf{E_0}\rvert_{\max}$
400	$6.59 \cdot 10^{-2}$	38.430	0.08
500	2.920	25.081	1
800	$8.53 \cdot 10^{2}$	22.601	$2.21 \cdot 10^{2}$
1000	$1.377 \cdot 10^{5}$	20.713	$2.66 \cdot 10^{4}$
1500	$2.171 \cdot 10^{6}$	16.588	$2.15 \cdot 10^{5}$
2000	$1.583 \cdot 10^{7}$	13.019	$7.58 \cdot 10^{5}$
2500	$7.160 \cdot 10^{7}$	10.334	$1.71 \cdot 10^{6}$
6000	$1.671 \cdot 10^{8}$	4.278	$2.83 \cdot 10^{5}$

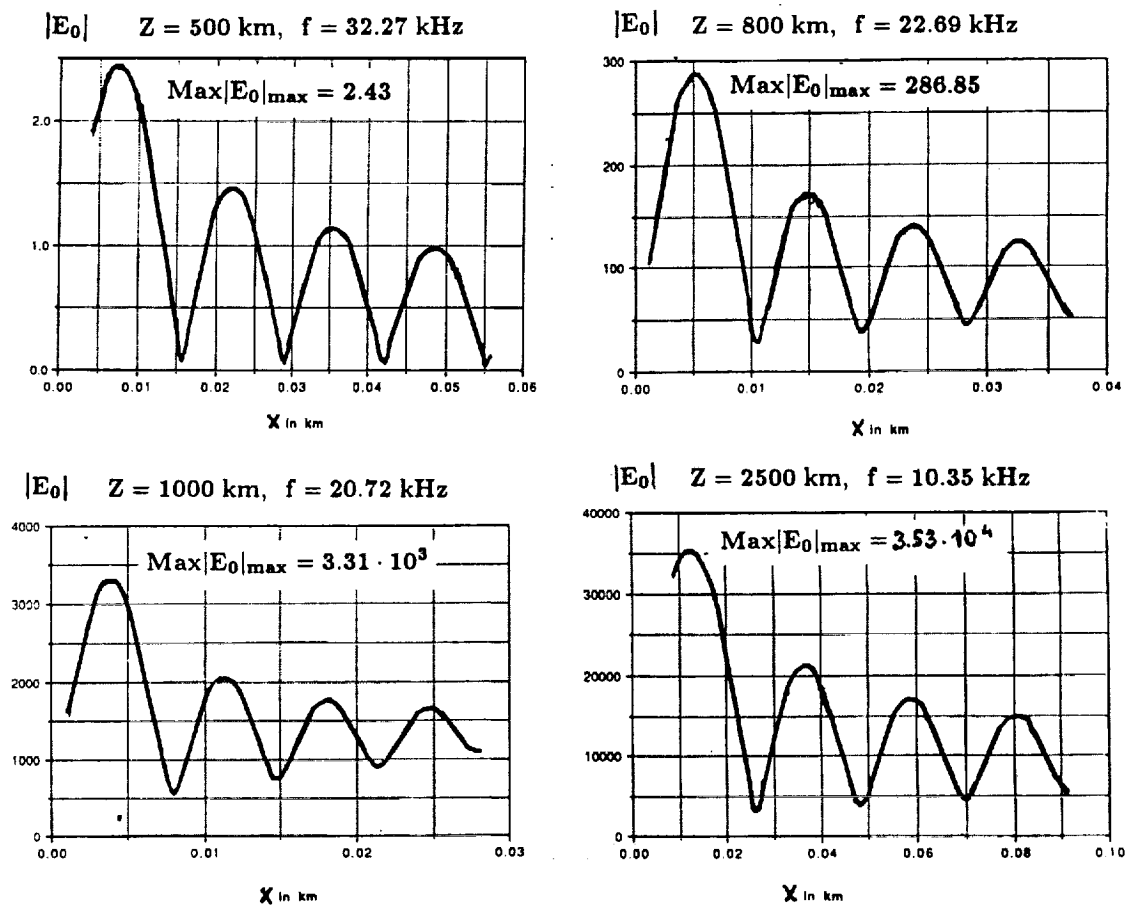

Fig 5. Dependencies of the Axis field modul $|E_0|$ on distance **x** from the magnetic field line $\mathbf{B_0}$ at different altitudes Z of the ionosphere at fixed frequencies.

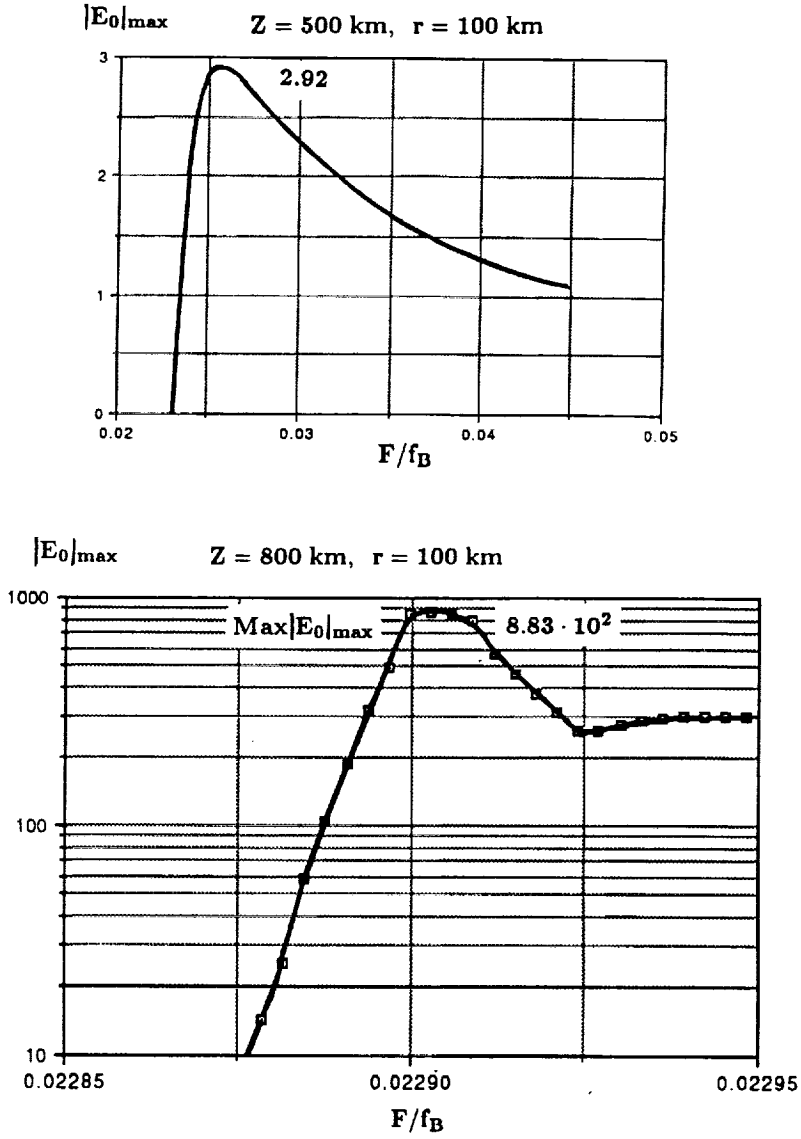

Fig 6. Frequency dependencies of the maximal values of $|E_0|_{max}$ (see Fig.5) at $Z = (800,\ 1000)\ km$.

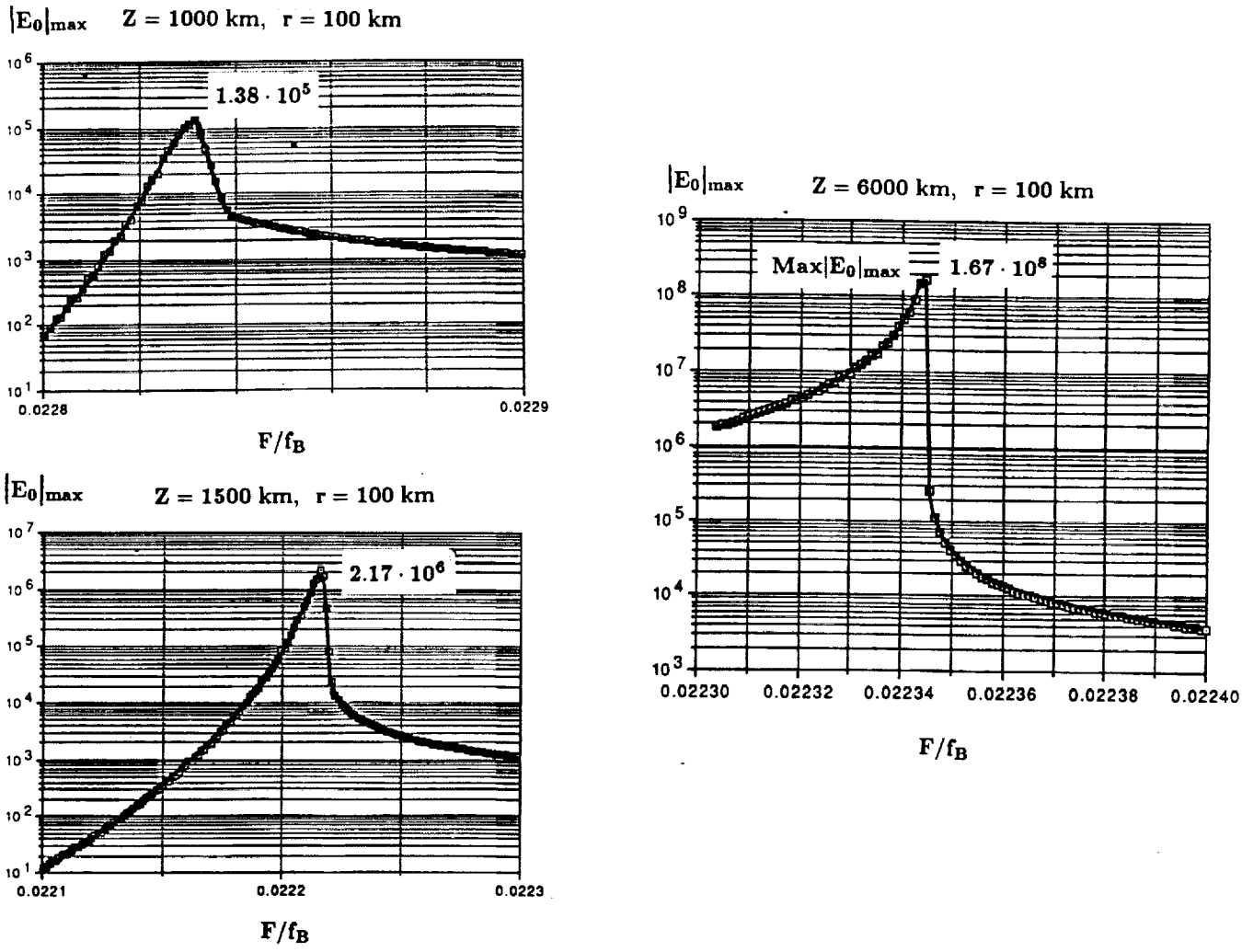

Fig 7. The same as on Fig.6 at Z = (1000, 1500, 6000) km.

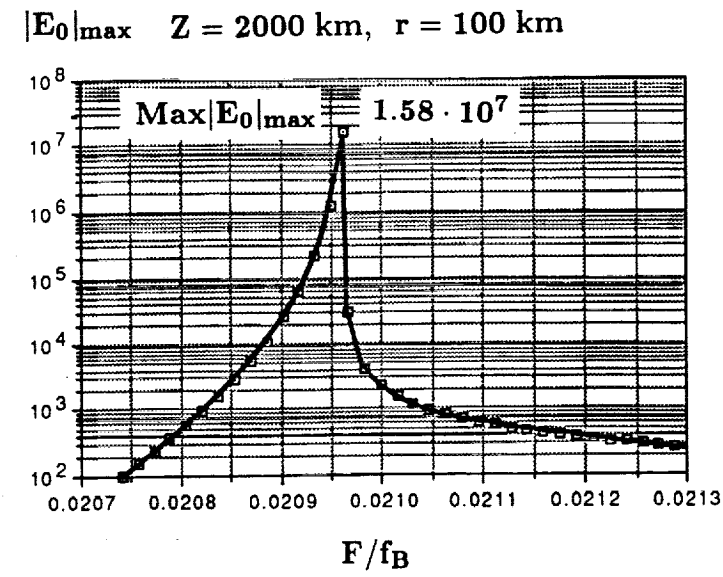

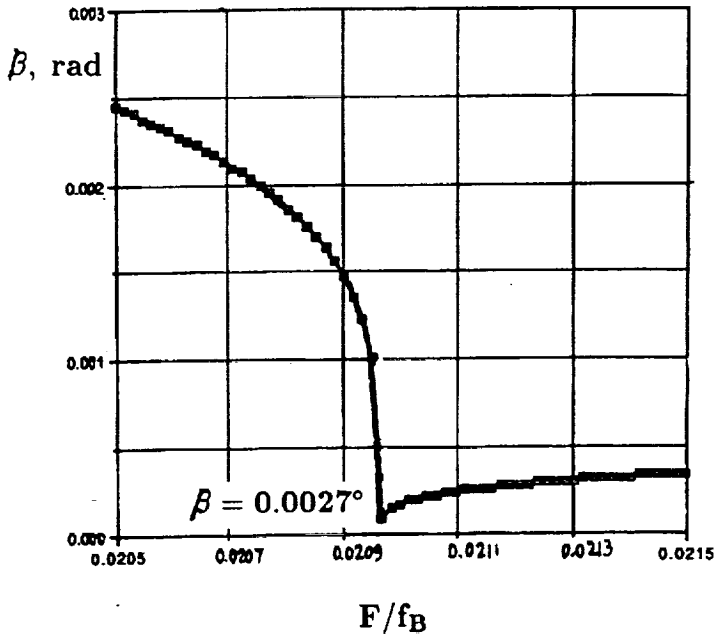

Fig 8. Frequency dependencies of $|E_0|_{max}$ and of the ray direction angle β at $Z = 2000\ km$.

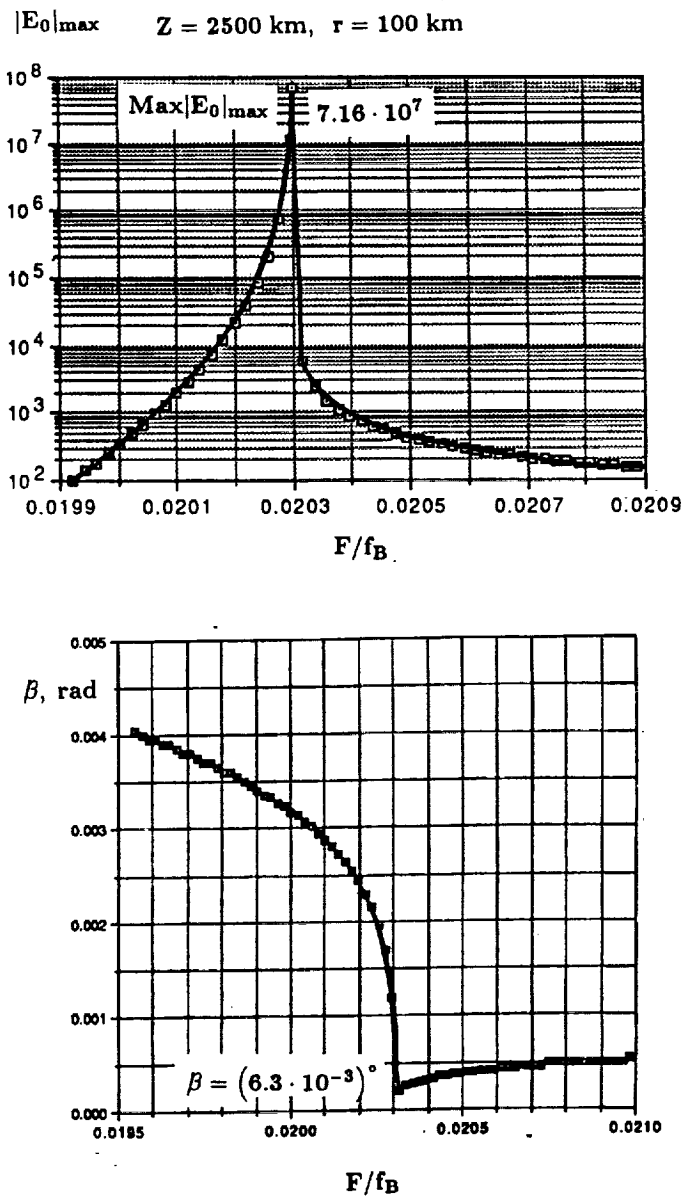

Fig 9. The same as on Fig.8 for $Z = 2500\ km$.

Fig.10

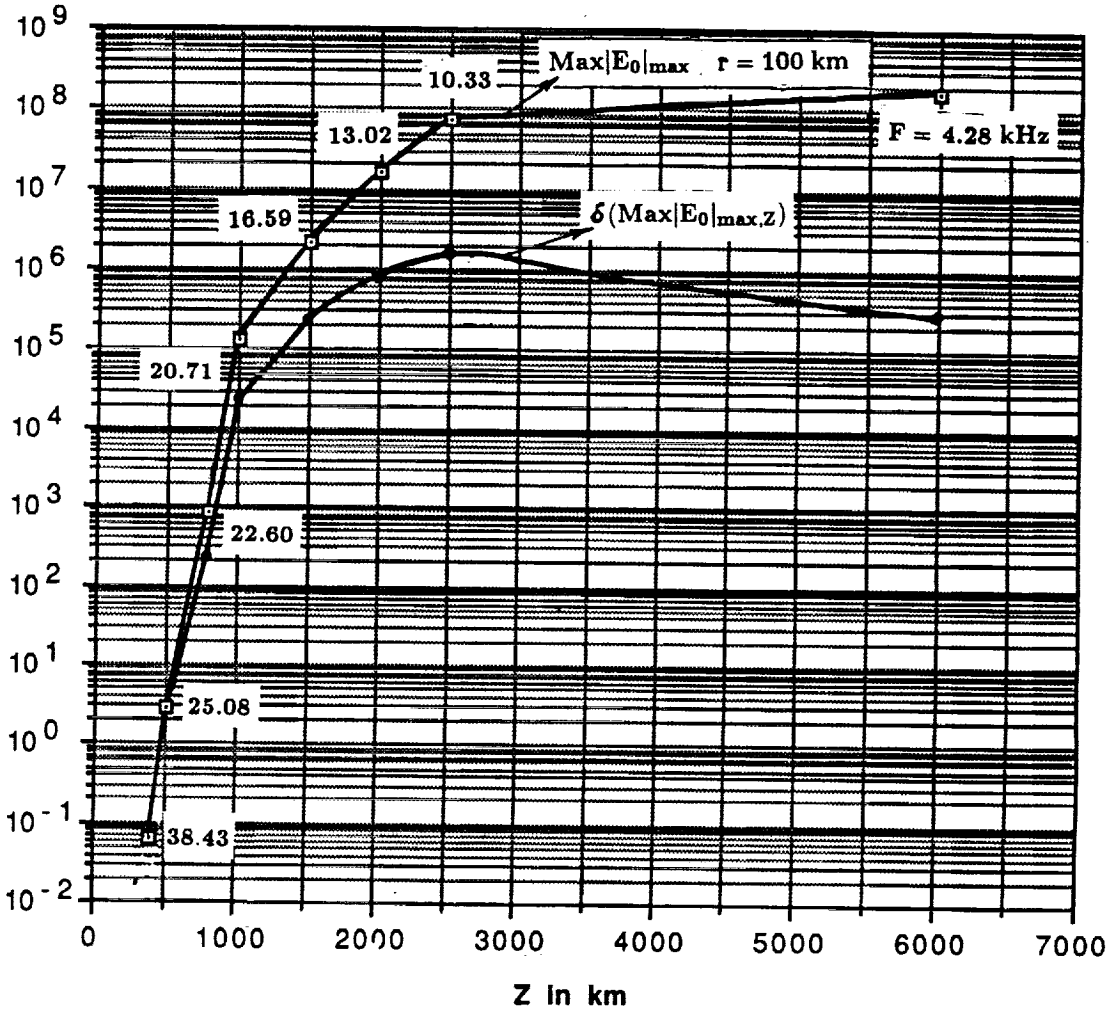

Fig 10. Altitude dependencies of the maximal values $Max|E_0|_{max}$ and of their normalized values $\delta(Max|E_0|_{max})$ to $Z = 500\ km$ (see (21)).

III. Nonlinear heating of a magnetoplasma by an electric field $\mathbf{E}e^{i\omega t}$.

It was noted above that the nonlinear theory of a magnetoplasma heating under the action of an electric field $\mathbf{E}e^{i\omega t}$ was recently extended by the author (see Alpert, 1990 [6], 1991 [8]). In connection with the Active mission, theoretical calculations were performed on the basis of this theory for a realistic altitude model of the ionosphere and in which includes frequencies of the VLF and LF bands $F = (1 - 16)\ kHz$ of this mission. The appropriate results of the numerical calculations are presented in this section. The analytical formulae used by some of these calculations are given below. However, a sufficiently full study of this problem is possible only by a computer, because of the big completeness of the solution of two interconnected systems of linear equations. For this purpose, a special computer programme was developed by Robert Estes, and part of numerical calculations were done in collaboration with him.

III.1 Microscopic theory, formulae. Limits of its applicability.

In the microscopic (hydrodynamic) approximation, to calculate the temperatures of a magnetoplasma, containing three kind of particles: electrons $< e >$, ions $< i >$ and one kind of neutral particles $< n >$, the following two interconnected linear systems of differential equations of the first order should be solved:

$$\begin{aligned}
\frac{d\mathbf{V}_e}{dt} &= -\frac{e\mathbf{E}}{m} - \frac{e}{mc}(\mathbf{V}_e \times \mathbf{B}) - \nu_{ei}(\mathbf{V}_e - \mathbf{V}_i) - \nu_{en}(\mathbf{V}_e - \mathbf{V}_n), \\
\frac{d\mathbf{V}_i}{dt} &= \frac{e\mathbf{E}}{M} + \frac{e}{Mc}(\mathbf{V}_i \times \mathbf{B}) + \frac{m}{M}\nu_{ei}(\mathbf{V}_e - \mathbf{V}_i) - \nu_{in}(\mathbf{V}_i - \mathbf{V}_n), \\
MN_n\frac{d\mathbf{V}_n}{dt} &= mN_e\nu_{en}(\mathbf{V}_e - \mathbf{V}_n) + MN_i\nu_{in}(\mathbf{V}_i - \mathbf{V}_n), \qquad (22)
\end{aligned}$$

and

$$\begin{aligned}
\frac{dT_e}{dt} &= -\frac{2}{3}e\mathbf{V}_e\cdot\mathbf{E} - \delta_{ei}\nu_{ei}(T_e - T_i) - \delta_{en}\nu_{en}(T_e - T_{no}) \\
\frac{dT_i}{dt} &= \frac{2}{3}e\mathbf{V}_i\cdot\mathbf{E} + \delta_{ei}\nu_{ei}(T_e - T_i) - \delta_{in}\nu_{in}(T_i - T_{no}) \\
N_n\frac{dT_n}{dt} &= N_e\delta_{en}\nu_{en}(T_e - T_{no}) + N_i\nu_{in}\delta_{in}(T_i - T_{no}) \qquad (23)
\end{aligned}$$

The following notation are used in (1) and (2):

$\mathbf{V}_e$, $\mathbf{V}_i$ and $\mathbf{V}_n$, T_e, T_i and T_n, being as functions of $\mathbf{E}$ and ω are the velocities and temperatures of all the kind of particles;

N_e, N_i and N_n, and m, $M_i = M_n = M$ are the densities of these particles;

δ_{en}, δ_{ei}, δ_{in} are, respectively, the energy lost by the electrons due to their chaotic collisions with the neutral particles and ions and energy lost by the ions due to their collisions with the neutral particles (the values $\delta_{en} \simeq \delta_{ei} \simeq 2\cdot 10^{-3}$ and $\delta_{in} \simeq 1$ were used).

The collision frequencies between all the kinds of particles are:

$$\begin{aligned}
\nu_{ei}(E,\omega) &= \nu_{ei,0}\left(\frac{T_{e0}}{T_e(\mathbf{E})}\right)^{3/2}\cdot\frac{\ln\left[0.37\frac{T_e(\mathbf{E})}{e^2N_e^{1/3}}\right]}{\ln\left[0.37\frac{T_{e,0}}{e^2N_e^{1/3}}\right]}, \\
\nu_{en}(E,\omega) &= \nu_{en,0}\left(\frac{T_e(\mathbf{E})}{T_{e,0}}\right)^{1/2}, \\
\nu_{in}(E,\omega) &= \nu_{in,0}\left(\frac{T_i(\mathbf{E})}{T_{i,0}}\right)^{1/2}. \qquad (24)
\end{aligned}$$

Besides, before the action of the field, at the moment $t = 0$, the magnetoplasma is isothermal $T_{e0} = T_{i0} = T_{n0}$, and quasi neutral $N_{e0} = N_{i0}$.

The analytical formulae of $\mathbf{V}$ of the solution of the system of equations (21) - (23) are transparent only when the dependence of the collision frequencies on the electric field is not taken into account - i.e. by the *approximation*

$\nu = const.$ These formulae are given in [6], [8] when $\frac{dT_n}{dt} = 0$, i.e. when the third equation of (2) is not taking into account, $T_n = T_{n0}$. They become much simpler when the angle Θ between the electric field $\mathbf{E}$ and magnetic field $\mathbf{B_0}$ is zero and $\mathbf{E} \parallel \mathbf{B_0}$. The following coordinate system is used here:

$$\begin{aligned} B_x &= B_y = 0 \quad \mathbf{B_0} \parallel \mathbf{z}, \\ E_x &= 0, \quad E_y = E\sin\Theta, \quad E_z = E\cos\Theta \end{aligned} \tag{25}$$

Nevertheless, these analytical formulae are still sufficiently complicated when the angle $\Theta \neq 0$. Therefore, numerical calculations with those formulae were also done by the computer. By learning of these formulae it was discovered that the used in the literature formulae (see, for examples, Gurevich, 1978 [10]), when $B_0 \neq 0$ can be used only when

$$\omega^2 \gg \omega_L^2 + \nu_e\nu_{in}, \tag{26}$$

where ω denotes the angular frequencies.

By the computer calculations, it was found that the influence of the magnetic field becomes sufficiently effective only by $\Theta \geq 30°$ (see below). Therefore, the formulae for an *isotropic plasma* ($B_0 = 0$, $\Theta = 0$) may be often used for evaluation of the velocities and temperatures $T(E)$. Namely

$$\begin{aligned} V_e &= -\frac{eE}{m\nu_e} \cdot \frac{\left(1 - i\frac{\omega}{\nu_{in}}\right)\left(1 - \frac{\omega^2}{\nu_e\nu_{in}} + i\frac{\omega}{\nu_{in}}\right)}{\left(1 - \frac{\omega^2}{\nu_e\nu_{in}}\right)^2 + \frac{\omega^2}{\nu_{in}^2}}, \\ V_i &= -\frac{eE}{M\nu_e} \cdot \frac{\nu_{en}}{\nu_{in}} \cdot \frac{\left(1 - \frac{n\nu_{en}}{\omega + in\nu_{in}} - i\frac{\omega}{\nu_{en}}\right)\left(1 - \frac{\omega^2}{\nu_e\nu_{in}} + i\frac{\omega}{\nu_{in}}\right)}{\left(1 - \frac{\omega^2}{\nu_e\nu_{in}}\right)^2 + \frac{\omega^2}{\nu_{in}^2}}. \end{aligned} \tag{27}$$

Their real parts are

$$\begin{aligned} R_e(V_e) &= \frac{-eE}{m} \cdot \frac{\nu_e\omega^2 - \nu_{in}(\omega^2 - \nu_e\nu_{in})}{(\omega^2 - \nu_e\nu_{in})^2 + \nu_e^2\omega^2}, \\ R_e(V_i) &= \frac{-eE}{M} \cdot \frac{\nu_e\omega^2 - \nu_{en}(\omega^2 - \nu_e\nu_{in})}{(\omega^2 - \nu_e\nu_{in})^2 + \nu_e^2\omega^2}, \end{aligned} \tag{28}$$

and

$$V_n = \frac{V_e + \frac{\nu_{in}}{\nu_{en}}\frac{M}{m}\nu_i}{1 + \left(\frac{\nu_{in}}{\nu_{en}}\frac{M}{m} - \frac{i\omega}{n\nu_{en}}\right)\frac{M}{m}}, \tag{29}$$

where $\nu_e = \nu_{ei} + \nu_{in}$ and $n = \frac{N_e}{N_n}$. Again, it was found that the formula

$$V_e = R_e(V_e) = \frac{-eE}{m} \cdot \frac{\nu_e}{\omega^2 + \nu_e^2} \tag{30}$$

used in the literature (see [5]) is effective only when

$$\omega^2 \gg (\nu_{ei} + \nu_{in})\nu_{in} \tag{31}$$

The formulae of the temperatures of all the particles consist of two parts. One is periodically changing in time at the double frequency 2ω of the electric field $\mathbf{E}e^{i\omega t}$. The second part is stationary and is much larger than the depending on time part. The stationary temperatures $T(E)$ are of the most interest in this study. In an isotropic plasma ($\Theta = 0$), the stationary temperatures T_e and T_i are estimated in the approximation $\gamma = const$, $\frac{dT}{dt} = 0$, $T_n = T_{n0}$ by

$$\left(\frac{T_e(E,\omega)}{T_{n0}}\right)_{stat} = 1 + \frac{E^2}{E_h^2}\,. \tag{32}$$

and

$$\frac{T_i(E,\omega)}{T_{n0}} = 1 + \frac{E^2}{E_h^2}\left[1 + \frac{1}{\delta_e}\frac{\nu_{in}}{\nu_e}\left(1 + \frac{\nu_{en}}{\nu_{ei}}\right)\right]^{-1}\,, \tag{33}$$

where the squared characteristic field of this problem

$$E_h^2 = \frac{3m\delta_e\nu_e^2 T_{n0}}{e^2} \cdot \frac{A(\nu,\omega)}{A_1(\nu)}\,, \tag{34}$$

and

$$A_1(\nu) = \frac{\nu_e + \frac{\nu_{in}}{\delta_e}\left(1 + \frac{\nu_{en}}{\nu_{ei}}\right)}{\nu_{en} + \frac{\nu_{in}}{\delta_e}\left(1 + \frac{\nu_{en}}{\nu_{ei}}\right)}\,, \tag{35}$$

$$A(\nu,\omega) = \frac{\left(1 - \frac{\omega^2}{\nu_e\nu_{in}}\right)^2 + \frac{\omega^2}{\nu_{in}^2}}{\left(1 - \frac{\omega^2}{\nu_e\nu_{in}}\right) + \frac{\omega^2}{\nu_{in}^2}} = \left[\nu_e R_e\{V_e\}\right]^{-1}\,. \tag{36}$$

By comparison of (32) and (33) we can see that the temperature $T_i(E_0,\omega)$ of the ions is smaller than the temperature $T_e(E_0,\omega)$ of the electrons. However, really in the ionosphere this is remarkable only at the altitudes $Z \leq (100 \rightarrow 200)\ km$. At $Z \geq 200\ km$, $T_i(E_0,\omega) \simeq T_e(E_0,\omega)$.

The formulae (32) to (36) were used for some calculations of the temperatures. However, an important part of these calculations was done by computer programme. This helped us to learn the limits of the suitability - applicability of the approximations:

$$\begin{aligned} \nu &= const, \quad \frac{dT_n}{dt} = 0, \quad T_n = T_{n0}, \\ \nu &= \nu(\mathbf{E},\omega), \quad \frac{dT_n}{dt} \neq 0, \quad T_n = T_n(\mathbf{E},\omega). \end{aligned} \tag{37}$$

These results are given in the next section. However, first of all, let us single out here what, in general, are the limits of applicability of the microscopic hydrodynamic theory of the heating of a magnetoplasma under the action of an periodically alternative electric field, used widely in the literature.

It is obvious, that in a collisional medium, without any other losses, the system of the equations (2) of the derivatives $\frac{dT_e}{dt}$, $\frac{dT_i}{dt}$ and $\frac{dT_n}{dt}$ has not a stationary solution. Indeed, its determinant $\Delta_3 = 0$. Even the temperature of the neutral particles is growing up continuously in time under the action of the electric field and becomes a source of heating of electrons and ions (see below Fig.17). By shortening of this system, namely, *assuming* that $\frac{dT_n}{dt} = 0$, $T_n = T_{n0}$, the solution of the shortened system of two equations becomes stationary because of additional source of losses of this process becomes the saved in the equations collisions ν_{en} and ν_{in} between the electrons and ions with the neutral particles. On Fig.11, the establishment in time of the temperature $T_e(E_0,\omega)$, calculated by the selfconsistent solution of the

full system of equations (22), and of the shortened system of equations (23) are shown for illustration. The approximation $\nu(E,\omega)$ was also used by this calculations, namely, the equations (3). It is seen that in the discussed case when $\frac{dT_n}{dt} \neq 0$, $T_n = T_{n0} \neq const$, the temperature $T_e(E,\omega)$ is reaching its stationary value in about 50 seconds. However, by solution of the full systems of these equations, when $\frac{dT_n}{dt} = 0$, the temperature is growing up all the time and almost linearly when $t > 1000$ *sec.*

A system of four equations (22), (23) characterize a full ionized magnetoplasma, namely: $N_e = N_i$, $\nu_{ei} \neq 0$, $N_n \simeq 0$, $\nu_{en} \simeq \nu_{in} \simeq 0$. This is the case closely realized in the magnetosphere. However, this system of equations has not a stationary solution too. It happened because the loss of the energy of the electrons accelerated by the electric field is equal to the energy transmitted by them to the ions. The determinant of this system $\Delta_2 = 0$. The temperatures T_e and T_i are growing up all the time.

Thus, the limits of applicability of the microscopic approximation used in many studies and here, by considering the behavior of all the temperatures T_e, T_i, and T_n by the two approximations: $\nu = const$ and $\nu(\mathbf{E},\omega)$ should be known. Especially it was important to search in this study the role of the neutral particles. The results of appropriate calculations are illustrated in the next section.

The heating of the magnetoplasma is accompanied and regulated, in addition to the collisions ν_{ei}, ν_{en} and ν_{in}, by many other processes. Their role should be of different degree. By a complete solution of this problem, they

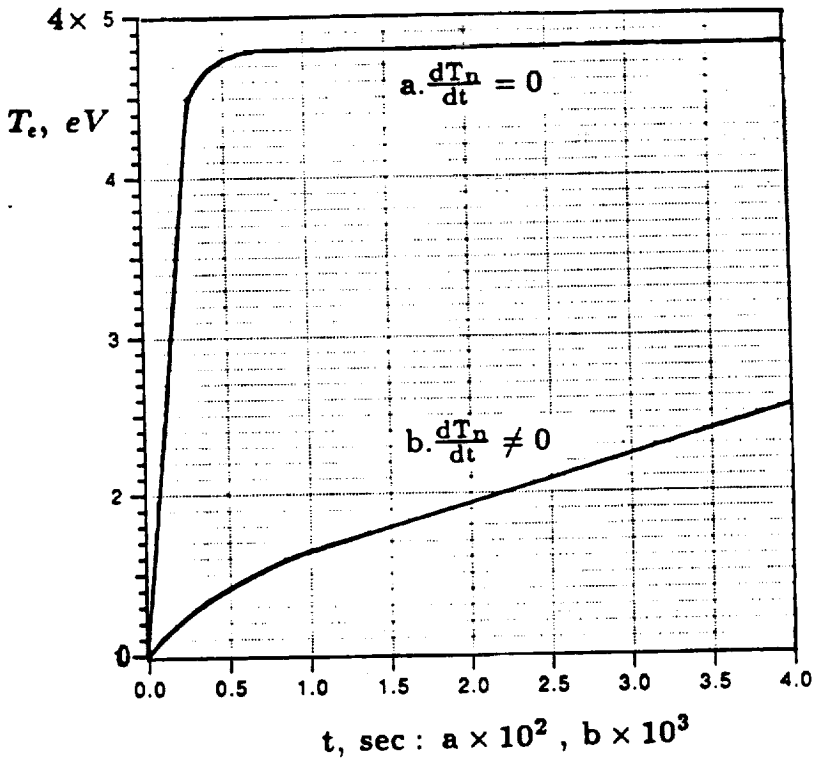

Fig 11. Establishment of the temperature $T_e(\mathbf{E}, \omega)$, $F = 1Hz$, $\Theta = 0$, $Z = 200\ km$. Approximation $\nu = \nu(\mathbf{E}.\omega)$.

should be taken into account. The general solution of this task will become stationary and the growth of the temperature can be stopped. However, it becomes a very complicated theoretical task. But, it seems that one of these most important processes is the *ionization* of the neutral particles *by the accelerated electrons* under the action of the electric field $\mathbf{E}_0 e^{i\omega t}$. Other losses of energy which can stop the growth of the temperature of the magnetoplasma are, for example:

the *thermal emission* of the constituent particles of the plasma i.e. the volume Stefan- Boltzman emission of the plasma,

the *heating kinetic losses* of the plasma, i.e. the *electron-electron* and *ion- ion* collisions ν_{ee} and ν_{ii} and possibly other kind of kinetic thermal losses which, in a sense, are similar to the Landau damping of e.m. waves in a plasma. Let us here only look at the ionization process of plasma by the accelerated electrons.

The velocity of the electrons becomes in the ionosphere, depending on the frequency ω and altitude Z, larger than the ionization potential E_i of the neutral particles. Namely, the thermal, chaotic velocity $v_e(\mathbf{E})$ plays the prime role by this process. It is considerably larger than the directed velocity $V_e(\mathbf{E})$. For instance, in an isotropic plasma

$$v_e(\mathbf{E}) = \left(\frac{2\kappa T_e(E_0,\omega)}{m}\right)^{1/2} \sim \frac{R_e\{V_e(\mathbf{E})\}}{\sqrt{\delta}} \sim 20 R_e\{V_e(\mathbf{E}) \qquad (38)$$

The ionization potential of the atomic hydrogen H_1 particles (they are the main constituent at the high altitudes of the ionosphere) $E_i = 13.54\ eV$. Therefore, the process of the ionization begins when $\mathbf{v_e}(\mathbf{E}) \geq 2.2 \cdot 10^8\ cm/s$. The *additional density* of the electrons $N_e(\mathbf{E})$ can become even considerably larger than the regular density of the plasma N_e when the amplitude of the electric field is rather small, even when $E_0 = (1-2)\ mV/m$.

Indeed, the cross-section $\sigma_e(E_i)$ of ionization of the atomic hydrogen increases rapidly with E_i up to a sharp maximum $\sigma_{e,max} \simeq (7-8)10^{-17}\ cm^2$ and then it is smoothly decreasing up to $\sigma_{e,stat} \simeq 2 \cdot 10^{-17}\ cm^2$ (Massy at al. 1969 [11]). At $Z = 300\ km$, for example, where the atomic hydrogen density $N_n \simeq 3 \cdot 10^9$, the production of the electrons

$$I_e = \sigma_e \cdot N_n \cdot v_e(\mathbf{E}) \geq (10\ to\ 50)\ s^{-1} \tag{39}$$

The additional ionization is described by the recombination equation

$$\frac{dN_e}{dt} = I_e N_e - \alpha_e N_e^2. \tag{40}$$

Growing up in time $N_e(t)$ reaches a maximum by $\frac{dN_e}{dt} = 0$ equal to $N = 10^9$, even if the coefficient of recombination $\alpha_e \sim 10^{-8}\ cm^3 \cdot s^{-1}$. However, at the discussed here altitudes Z, $\alpha_e < , \ll 10^{-8}$. Thus, under the action of the electric field, the surrounding plasma can become *full ionized.* As a result, the collision frequency between the electrons and ions $\nu_{ei}(\mathbf{E}) \propto N_e(\mathbf{E})/T_e(\mathbf{E})^{3/2}$ becomes very large. The growth of T_e is stopped very quickly because the electron concentration is very quickly increasing. Indeed, in the point of inflection of the time dependence of the $N_e(\mathbf{E}, t)$, where $\frac{d^2N_e}{dt^2} = 0$, $N_e = \frac{I_e}{2\alpha}$. Thus, at that point $\frac{dN_e}{dt} = \frac{I_e^2}{4\alpha_e}$ is very large (the value of α_e is very small) and the tangential of $N_e(\mathbf{E}, t)$ is almost vertical.

The discussion of all the noted above points in detail is beyond the frame of this study. It is even impossible to do this because many initial data are not known and may be found only by treatment of appropriate experimental data. It is also seen below that, in many cases, they are not of the decisive importance in the altitude region of the Active mission.

III.2 Altitude and frequency dependencies of the temperature in the ionosphere.

The numerical calculations of the temperatures were done for an ionosphere model given in Section II (see page 6). The frequency band was widened, namely, $F = (1 \ \ to \ \ 10^4)\ Hz$ and more because of the general interest to study the heating of the ionosphere and magnetosphere by ELF waves $0 < F < F_B$, F_B is the ion gyrofrequency. By the preliminary calculations, it was learned that the growth of the temperatures T_e and T_i with altitude is very large at frequencies $F = (1 \ \ to \ \ 100)\ Hz$ and becomes about $(10^2 - 10^3)$ and many times larger than the temperature of the initial plasma T_{n0}. Therefore, $F = 1\ Hz$ is used to characterize this band of frequencies. It illustrates more dramatically the region where it is necessary to stop in the theory the temperature growth by including additional losses of energy. The zone of ionization by the accelerated electrons is marked on the plots by a line and vertical arrows. Besides, it was learned that in frequency band $F > (10^2 \ \ to 10^4)\ Hz$ and more, the altitude dependencies of the temperature are qualitatively the same, therefore, the frequency $F = 1000\ Hz$ was used to characterize this frequency band. The altitude temperature dependence on this frequency is sufficiently typical for this frequency band. These two frequencies are used also to characterize the angle Θ dependence of the temperatures. Let us remind here that Θ is the angle between the electric $\mathbf{E}$ and magnetic $\mathbf{B_0}$ fields.

a. Numerical results. Approximations $\nu = const$, $\nu = \nu(E, \omega)$.

Altitude dependencies T_e/T_{n0} and T_i/T_{n0} of the electron and ion temperatures for $\Theta = 0$, $F = 1\ Hz$ and $F = 1000\ Hz$ are shown on Fig.12. They were

calculated by the two approximations $\nu = const$ and $\nu_e = \nu(T) = \nu(\mathbf{E},\omega)$ (see (24)) by the selfconsistent solution of the system of equations (22) and shortened system of equations (23) when $\frac{dT_n}{dt} = 0$, $T_n = T_{no}$. Altitude dependencies by approximation $\nu = const$, $\frac{dT_n}{dt} = 0$, $T_n = T_{n0}$ are also shown: for $\Theta = 0$ and four different frequencies $F = (1 \ \ and \ \ 100)\ Hz$, $F = (10^3 \ \ and \ \ 10^4)\ Hz$ on Fig.13, for $F = 1\ Hz$ and angles $\Theta = (0,\ 30,\ 66,\ 75,\ 85\ 90)^\circ$ on Fig.14, and for $f = 10^3\ Hz$ and angles $\Theta = 0^\circ$, $\Theta = 75^\circ$ calculated by the approximations $\nu = const$ and $\nu = \nu(T) = \nu(E,\omega)$ on Fig.15.

By examination of all these figures, it is seen the following:

1. The character of the altitude dependencies of the temperatures is different in the frequency bands $F = (1\ to\ 100)\ Hz$ and $F = (10^3\ to\ 10^4)\ Hz$. This is also seen from Fig.16, where frequency dependencies are shown at $Z = 300\ km$ for the approximations $\nu = const$, $\nu = \nu(\mathbf{E},\omega)$ when $\frac{dT_n}{dt} = 0$, $T_n = T_{n0}$.

2. The temperatures of the electrons T_e and ions T_i are growing up quickly on both frequencies. They become equal in the altitude region $Z \sim (200 - 250)\ km$. In this region $(T_e \ \ and \ \ T_i) \geq (10^2 - 10^3)T_{n0}$.

3. The quick growing of temperatures, when $F = 10^3\ Hz$ is slowed down and at $Z \sim 200\ km$ they have maxima by the approximation $\nu = \nu(E_0,\omega)$ and $\nu = const$.

4. At $Z \geq 300\ km$ the temperatures *are smaller* by the approximation $\nu = \nu(E_0,\omega)$ than by the approximation $\nu = const$.

5. The process of ionization by the accelerated electrons is acting almost in all the altitude region when $F = 1\ Hz$ and *does not play a role*,

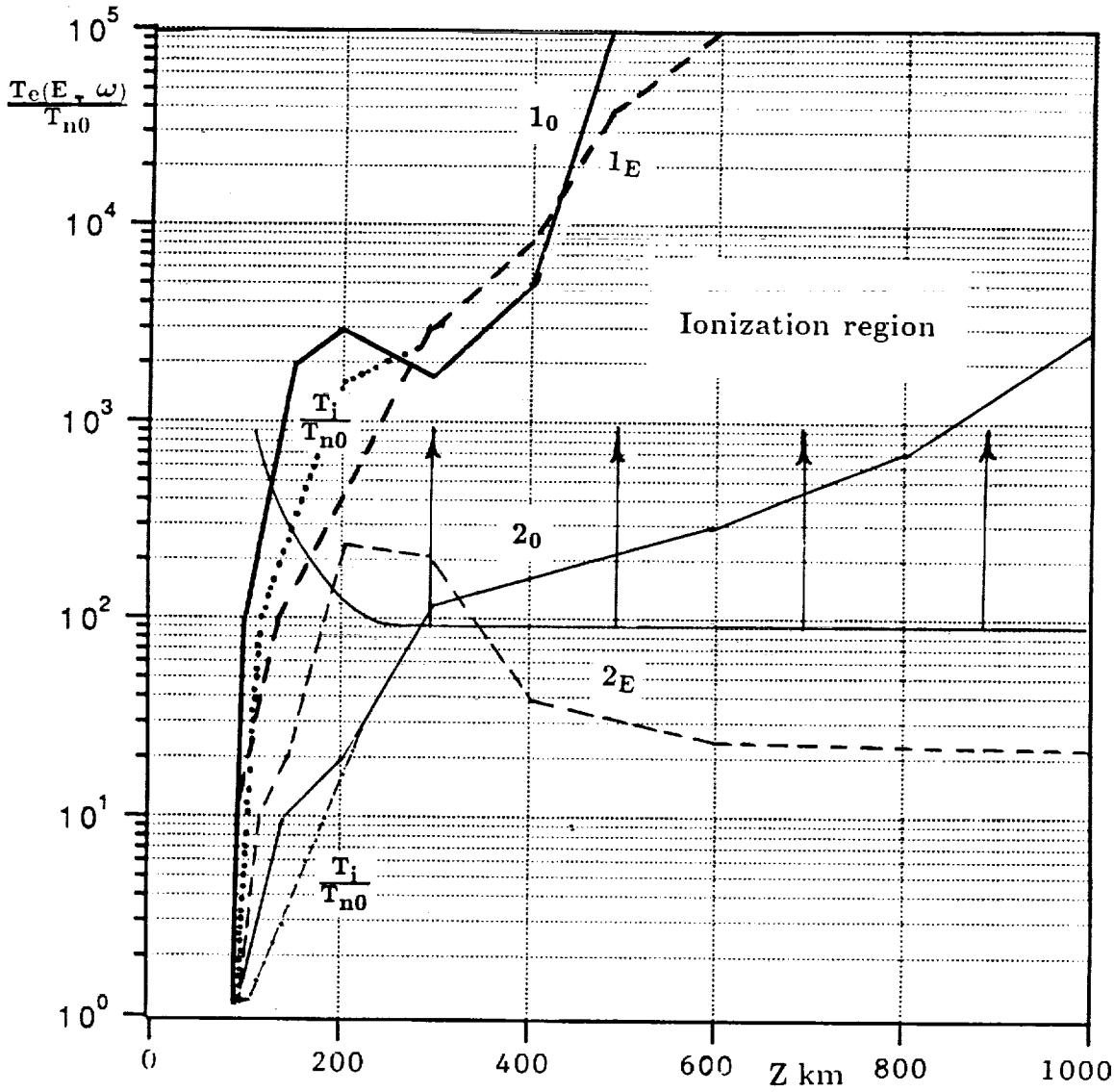

Fig 12. Altitude dependencies of T_e/T_{n0} and T_i/T_{n0}, $\Theta = 0$.
Approximation $\nu = const$, $F = (1 \ and \ 10^3)\ Hz \rightarrow 1_0,\ 2_0$.
Approximation $\nu = \nu(\mathbf{E}, \omega)$, $F = (1 \ and \ 10^3)\ Hz \rightarrow 1_E,\ 2_E$.

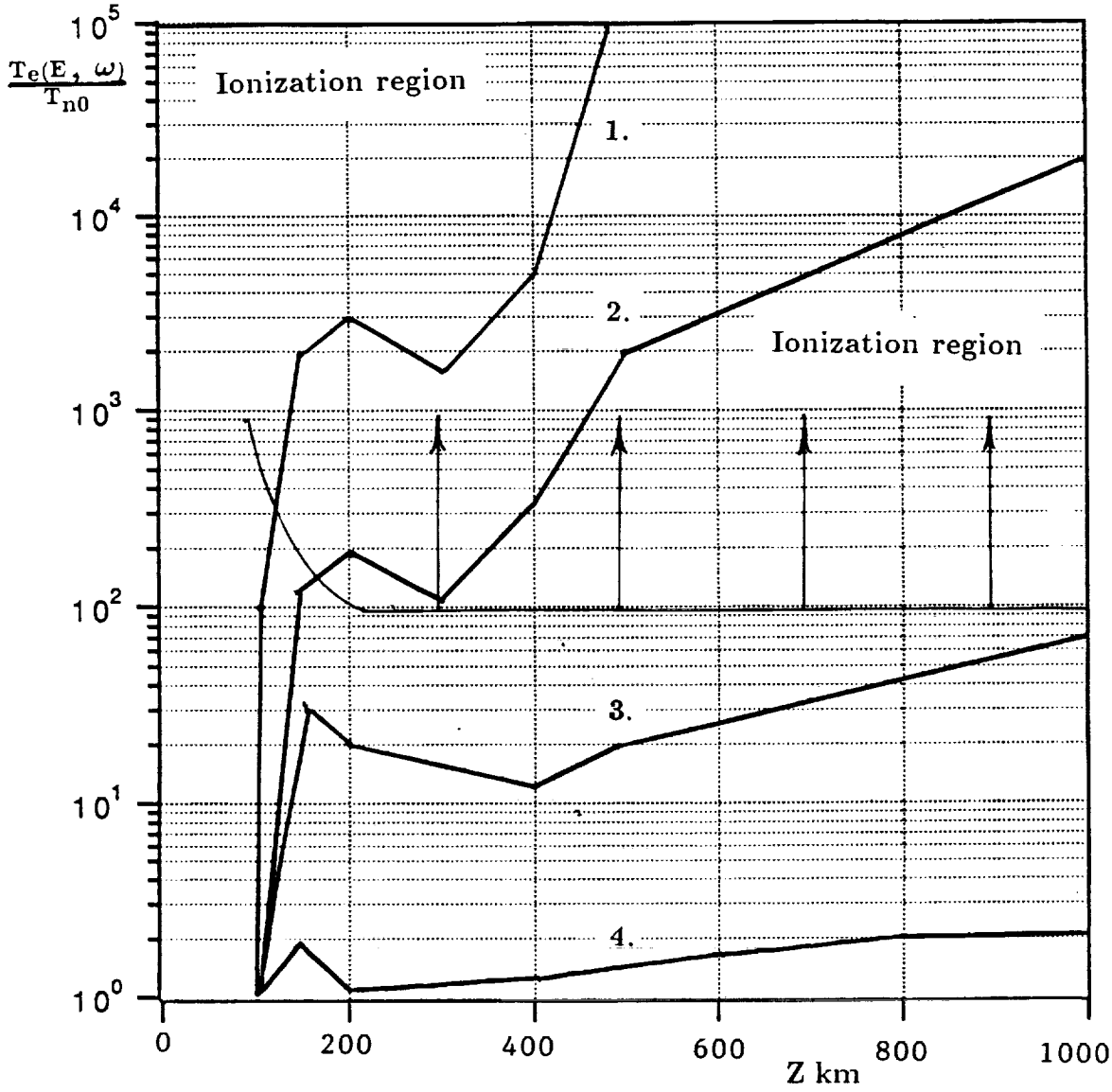

Fig 13. The same as on Fig.12 T_e/T_{n0}. Approximation $\nu = const.$ Frequencies $F = (0,\ 10^2,\ 10^3,\ 10^4)\ Hz \rightarrow 1.,\ 2.,\ 3.,\ 4.$

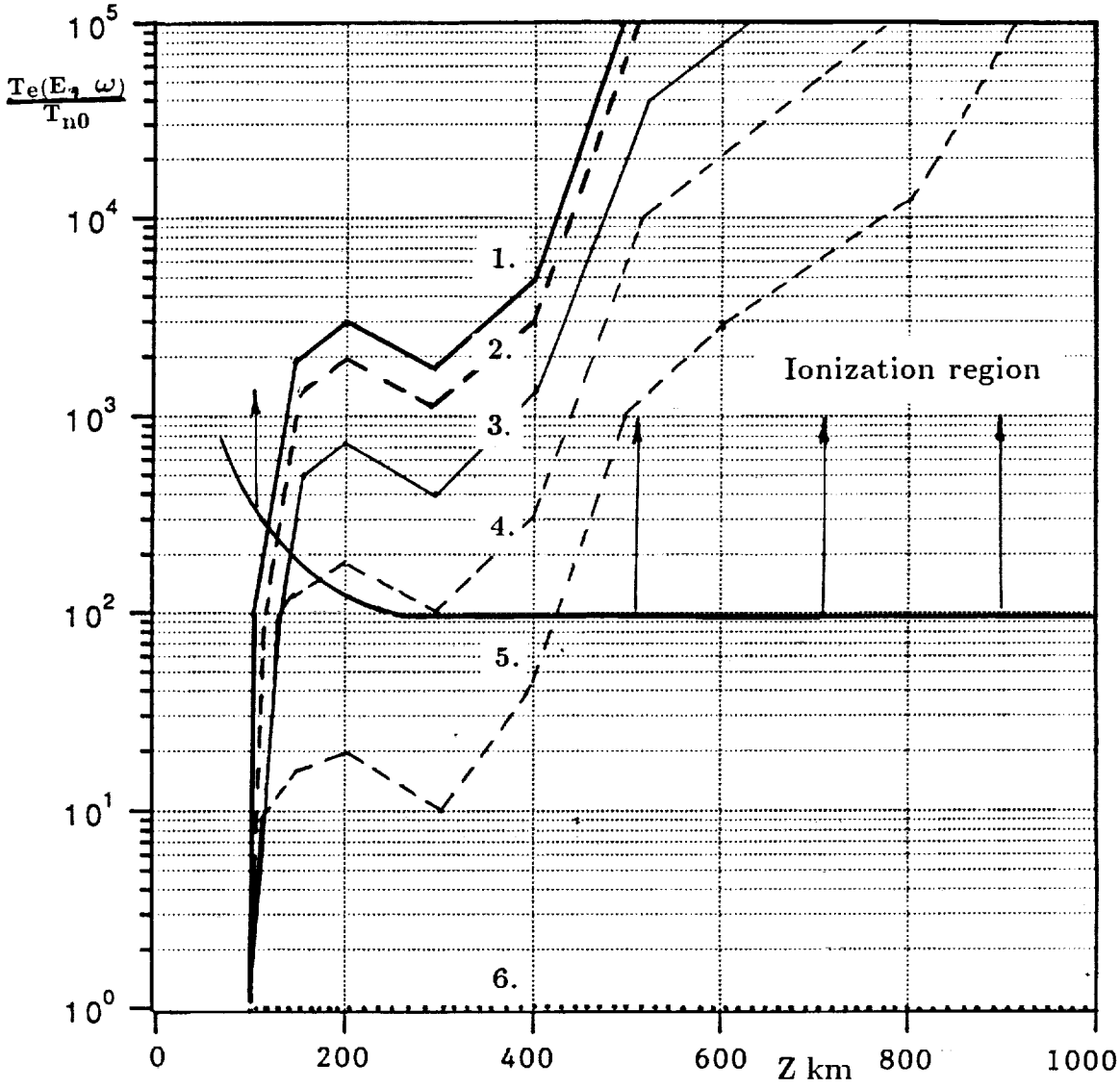

Fig 14. The same as on Fig.13. Angles between **E** and $\mathbf{B_0}$:
$\Theta = (0,\ 30,\ 60,\ 75,\ 85,\ 90)° \rightarrow 1,\ 2,\ 3,\ 4,\ 5,\ 6.$

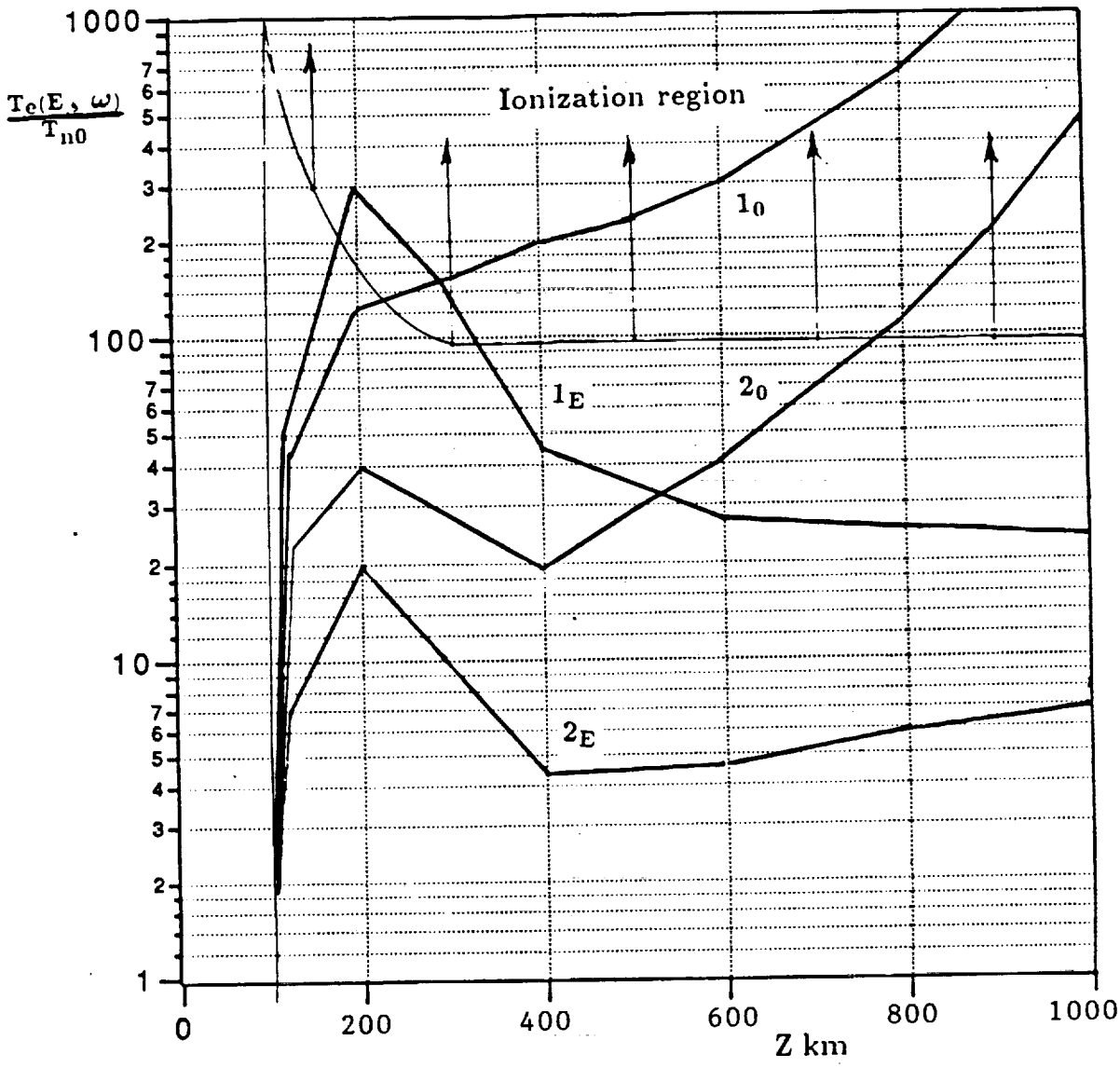

Fig 15. The same as on Fig.12, $F = 10^3\ Hz$.
Approximation $\nu = const$, $1_0 \rightarrow (\Theta = 0)$, $2_0 \rightarrow \Theta = 75°$.
Approximation $\nu = \nu(\mathbf{E}, \omega)$, $1_E \rightarrow (\Theta = 0)$, $2_E \rightarrow \Theta = 75°$.

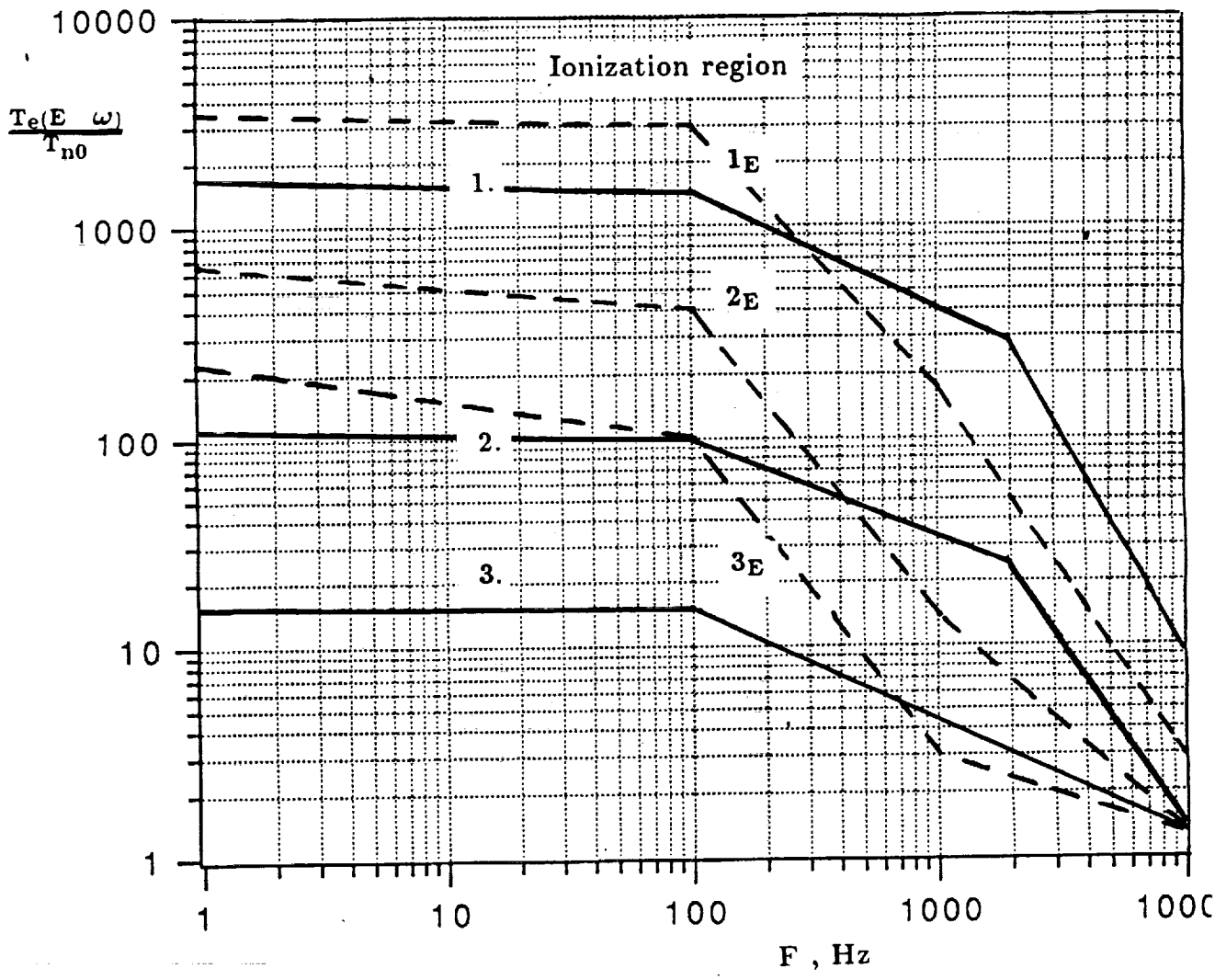

Fig 16. Frequency dependencies of $T_e(\mathbf{E},\omega)/T_{n0}$, $Z = 300\ km$
Approximation $\nu = const$, $\Theta = (0,\ 75,\ 85)° \rightarrow 1.,\ 2.,\ 3.$
Approximation $\nu = \nu(\mathbf{E},\omega)$, $\Theta = (0,\ 75,\ 85)° \rightarrow 1_E,\ 2_E,\ 3_E$.

when $F \geq 10^3\ Hz$, especially at $Z \geq 300\ km$. This process, namely $T_e(\mathbf{E},\omega) \geq 10^2 T_{n0}$ could be stopped by the theoretical calculations when $F = 1\ Hz$ already at the altitude $Z = (120 - 150)\ km$. This does not mean that the temperatures of the electrons and ions *can not become larger than the critical temperature* $T_{e,(i)}$ of ionization, let us say, of the atomic hydrogenH_1, which is equal to

$$T_{e,(i)} = 13.5\ eV = 1.16 \cdot 10^4 \cdot 13.5 = 1.57 \cdot 10^5,\ K°. \qquad (41)$$

To answer this question, theoretical studies must be done, taking into account losses of energy, in particular, noted in Section III.1.

6. The influence of the magnetic field becomes effective by angles $\Theta \geq 30°$. Thus the given above formulae for an isotropic plasma may be widely used for evaluation of the temperatures T_e and T_i in a magnetoplasma.

b. $\frac{dT_n}{dt} = 0$ and $\frac{dT_n}{dt} \neq 0$.

The calculations given in Section IIIa are in general confirmed by examination of the results of calculations of the temperature by selfconsistent solution of the full systems of equations (23) and (24), i.e. when $\frac{dT_n}{dt} \neq 0$, $T_n = T_n(\mathbf{E},\omega) \neq T_{n0}$. These results of calculations are illustrated by Fig.17. Not to overload this figure, only the T_e and T_n dependencies are given in it. The main new important characteristics of these dependencies, in addition to the given above 6 points, are the following:

1. The temperature T_n of the neutral particles is *growing up* very quickly at altitudes $Z > 200\ km$. It approaches the temperature T_e of the electrons at $Z > (400 - 500)\ km$ and *becomes close to* T_e similarly to the temperature of ions, T_i.

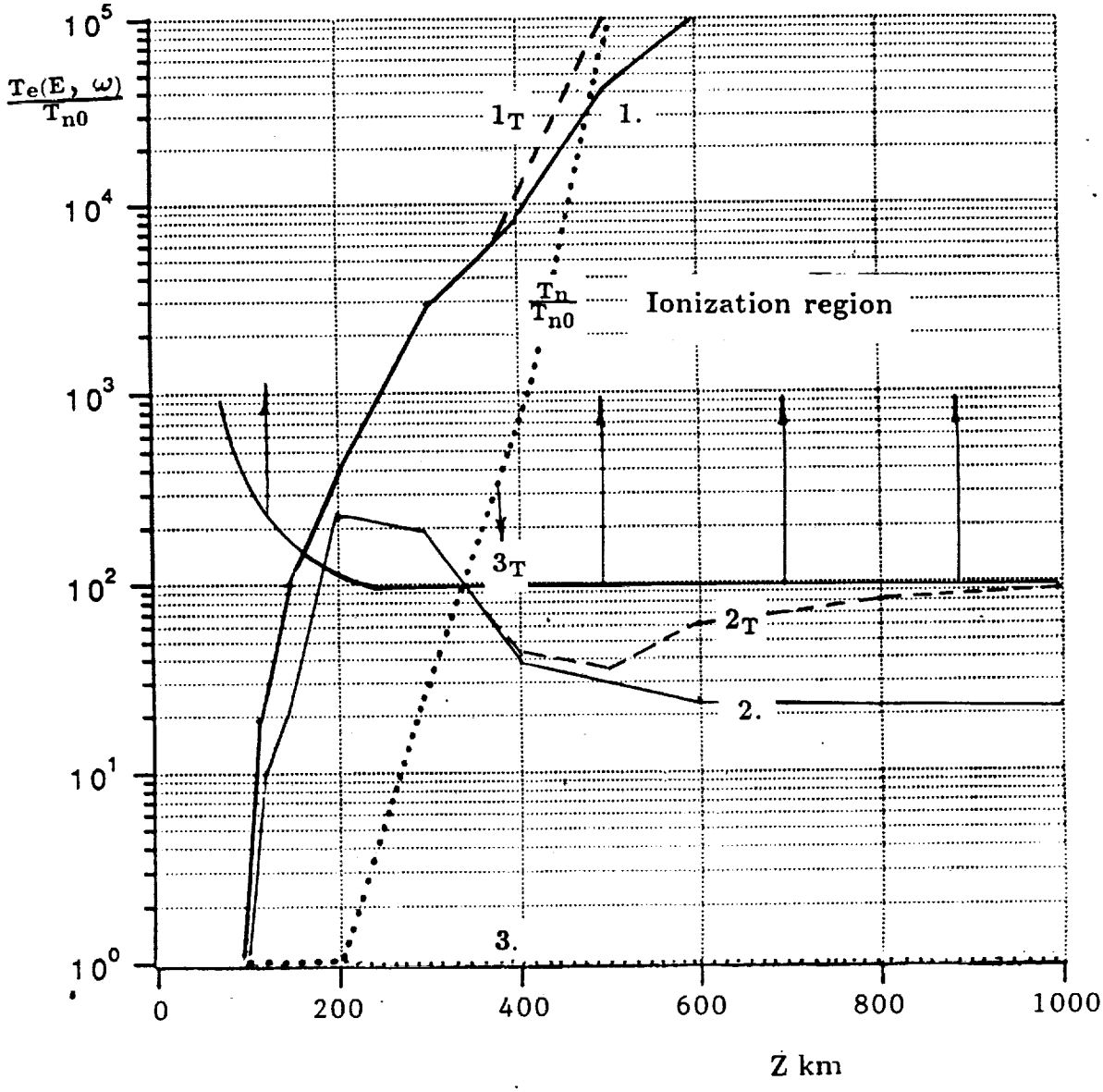

Fig 17. Altitude dependencies of the temperatures.
Approximations $\nu = \nu(\mathbf{E}, \omega)$, $\Theta = 0$.
$T_e(\mathbf{E},\omega)/T_{n0}$: $F = 1\ Hz$, **1.** $\rightarrow \frac{dT_n}{dt} = 0$, $\mathbf{1}_T \rightarrow \frac{dT_n}{dt} \neq 0$,
$F = 10^3\ Hz$, **2.** $\rightarrow \frac{dT_n}{dt} = 0$, $\mathbf{2}_T \rightarrow \frac{dT_n}{dt} \neq 0$,
$F = 1\ Hz$, **3.** $\rightarrow \frac{dT_n}{dt} = 0$, $\mathbf{3}_T \rightarrow \frac{dT_n}{dt} \neq 0$.

2. At the altitudes $Z > 400\ km$, the temperatures T_e *are larger* on both frequencies by the approximation $\frac{dT_n}{dt} \neq 0$ than by the approximation $\frac{dT_n}{dt} = 0$.

3. At least at $Z \geq 300\ km$, the heating of the neutral particles becomes a source of the heating of the electrons and ions. The growth of T_n should be stopped, similarly to the case $\frac{dT_n}{dt} = 0$ at these altitudes.

4. In many cases, the *heating of the neutral part'cles is an important part* in the process of heating of the magnetoplasma.

Summary

Results of calculations of the moduli of the electric field $|E|$ generated by an electric dipole at different altitudes of the ionosphere $Z \sim (300\ to\ 2500)\ km$ up to the bottom of the magnetosphere $Z \sim 6000\ km$ and in the frequency range $F_B \ll F < f_B$ are given. It is supposed that the source of this field is placed on a satellite, moving on an elliptical orbit which crosses this altitude region of the magnetoplasma. The electric field is recorded on another Sub-satellite moving around the source at distances of (10-s to $\sim 100\ km$) or a little more. The linear theory for a homogeneous medium may be used for treatment of the experimental data. The altitude frequency and angle dependencies of the field are studied in all the regions of their largest enhancement. They are the Axis field $|E_0|$, $\beta \sim 0$, close to the direction of the Earth's magnetic field line $\mathbf{B_0}$, the fields $|E_{St}|$ and $|E_{ResSt}|$ in the Storey cones, $\beta \sim (0\ to\ 10 - 20)\ degrees$, the Resonance cone field $|E_{Res}|$, $\beta \sim (0\ to\ 90)\ degrees$; β is the ray direction angle. The Axis field $|E_0|$ is studied here in detail. It is the most interesting and important peculiarity of this problem. The fields $|E_{St}|$, $|E_{RevSt}|$, and $|E_{Res}|$ are increased by a factor

of $(10\ to\ 10^5)$ and more by approaching the low hybrid frequency. The value of $|E_0|$ is increasing at the altitude $(500-2500)\ km$ about 10^6 times and it is *concentrated* in angles $\Delta\beta < 10^{-1}\ degrees$. These waves produce formations *similar to laser beams.* In the used model of the ionosphere, it should happen in our case in the frequency range $F \sim (20\ to\ 10)\ kHz$.

The extended recently microscopic theory of heating of the magnetoplasma is used to calculate the temperatures in the ionosphere. Adequate formulae and some numerical results are given, particularly, based on the self-consistent solution of a system of equations of the derivatives velocities $\frac{d\mathbf{V}_{e,i,n}}{dt}$ and of the temperatures $\frac{dT_{e,i,n}}{dt}$. All kind of collision frequencies between the constituents of the magnetoplasma ν_{ei}, ν_{en} and ν_{in} are taken into account. Numerical results illustrate the altitude and frequency dependencies of the temperature $T_{e,i,n}$ in the frequency band $F = (1-10^4)\ Hz$ and altitude range $(100\ to\ 10^3)\ km$. The heating of the ionosphere is growing up very quickly, with altitude. The temperatures reach the ionization potential even when the electric field $|E|$ is about some units of mv/m. At $Z \simeq (150-200)\ km$, $T_e \geq 10^2 T_{n0}$ in this region.

It is very important to investigate in detail the studied in this report problems by experiments on satellites. The treatment of the experimental data by the given above results of calculations will help both, to understand more the physics of different processes in the magnetosphere and also to improve the existing theories of these phenomena.

References

1. Alpert Ya.L., 1989. Proposal P2159-8-89 for NASA, Smithsonian Institution, Astrophysical Observatory.

2. Alpert Ya.L. & Moiseyev B.S., 1980a, Journ. Atm. Terr. Phys. **42**, 521.

3. Alpert Ya.L., Budden K.G., Moiseyev B.S. & Stott C.F., 1983, Phil.Trans. Roy. Soc., London **A 309**, 503.

4. Alpert Ya.L., 1980b, Journ. Atm. Terr. Phys., **42**, 205.

5. Alpert Ya.L., 1983, Ann. of NY Acad. Sci. **401**, 1.

6. Alpert Ya.L., 1988. Final Report for NASA, Contract NAS8-36809, Smithsonian Institution, Astrophysical Observatory.

7. Alpert Ya.L., 1991, IL Nouvo Cimento (in print).

8. Alpert Ya.L., 1991, American Institute for Aeronautics and Astronautics (in print).

9. Arbel E. & Felsen F.B., 1963, Electromagnetic Theory and Antennas, Part I, 421, edited by B.C. Jordon)Oxford, Pergamon Press).

10. Gurevich A.V., 1978. Nonlinear phenomena in the ionosphere, Springer Verlag, Berlin.

11. Massey H.S.W., Barchop E.H.S. & Gilbody H.B., 1969. Electronic and ionic impact phenomena, Second Edition, Oxford at the Caledon Press.